

Oligo-miocene subduction-related volcanism of the loyalty and three Kings ridges, SW Pacific: A precursor to Tonga-Kermadec arc

Agranier Arnaud ^{5,*}, Patriat Martin ¹, Mortimer Nick ², Collot Julien ³, Etienne Samuel ³, Durance Patricia ², Gans Phil ⁴

¹ Geo-Ocean, UMR6538 Univ Brest, CNRS, Ifremer, Plouzane, France

² GNS Science, Private Bag 1930, Dunedin 9054, New Zealand

³ Geological Survey of New Caledonia, DIMENC, BP M2, 98849 Nouméa, New Caledonia

⁴ Geological Sciences, University of California, Santa Barbara, USA

⁵ Geo-Ocean, UMR6538 Univ Brest, CNRS, Ifremer, Plouzane, France

* Corresponding author : Arnaud Agranier, email address : agranier@univ-brest.fr

Abstract :

The SW Pacific region contains several ridges and basins that are inferred to represent pre-Quaternary volcanic arcs and back-arc basins. The geology of these features is less well characterized than that of the active Tonga-Kermadec and Vanuatu arcs. We report new major and trace element, and Pb, Hf, Sr and Nd isotope data for 27 lavas dredged from the Loyalty and Three Kings ridges during the 2015 VESPA cruise of R/V l'Atalante. Low-K basalts were dredged from the seabed deeper than 3300 m, and high-K to shoshonitic suites from shallower ridge crests at 2000–3300 m. The samples are mainly basalts, with lesser trachybasalts, basaltic andesites, trachyandesites andesites, dacites, and one granite (anhydrous SiO₂ and K₂O + Na₂O range from ~47 to 64 and 1.5 to 11 wt% respectively). Trace element patterns allow discrimination of three geochemical signatures, identified as i) depleted, ii) transitional and iii) enriched, based on their light to heavy rare earth element (REE) ratios (with La/Sm ranging from 0.4 to 8). Depleted and transitional samples are basalts, featuring REE concentrations similar to MORB, but with high field strength element and large ion lithophile element contents, typical of back-arc basin basalts. The most enriched samples are basaltic andesites, andesites, trachyandesites and trachytes with island arc magma trace element signatures. Pb isotope ranges are limited (208Pb/204Pb ~38 to 39.8, 207Pb/204Pb ~15.51 to 15.64 and 206Pb/~17.9 to 20.1), while Hf isotopes display more diverse compositions (ϵ_{Hf} ranging from +7.7 to +14). Both Nd (ϵ_{Nd} = 2.8–9.3) and Sr (87Sr/86Sr = 0.7026–0.7048) isotopes are correlated with Hf data. Trace element and isotopic compositions can be explained in terms of mixing between three distinct geochemical endmembers in the mantle resembling DMM, HIMU and EM-2 sources. Our study confirms voluminous subduction-related magmatism on the Loyalty and Three Kings ridges, mostly of Late Oligocene – Early Miocene age. The issue of polarity of subduction to generate these rocks remains open, but the composition-space-time distribution of the igneous rocks can be explained in the context of SW Pacific geodynamics using a west-dipping Pacific slab model.

Highlights

- ▶ Late Oligocene–Miocene subduction-related magmatism on the Loyalty and Three Kings ridges.

Keywords : Zealandia, Loyalty Ridge, Three Kings Ridge, Igneous rocks, Geochemistry, Subduction

1 **1. Introduction**

2 The 95% submerged continent of Zealandia (Fig. 1A, Mortimer et al., 2017,
3 2020a) forms the western backstop to a region of active and inactive arcs and back-arc
4 basins in the southwest Pacific. The region has been volcanically active for more than
5 100 m.y. and hundreds of rift, hotspot, subduction and intraplate volcanoes have
6 erupted across the region. Subduction is currently active along the New Hebrides, and
7 Tonga-Kermadec trenches. Associated back-arc basins are the Havre, Lau and North Fiji
8 basins (Fig. 1A; Crawford et al. 2003; Collot et al., 2020). The tectonics, kinematics and
9 petrology of these features have been intensely studied, and processes and history are
10 very well characterized at the regional scale over the last 10 Ma (e.g. Pelletier et al.,
11 1998; Crawford et al., 2003). Less well studied is the older subduction record of the
12 southwest Pacific which is inferred to have started sometime in the Eocene or possibly
13 the Late Cretaceous (e.g. Crawford et al., 2003; Schellart et al., 2006; Matthews et al.,
14 2015; Collot et al., 2020). The eastward retreat of the Tonga-Kermadec trench has
15 allowed the geological records of remnant submarine arcs and unclosed back-arc basins
16 to be preserved, except where they have been subducted in southwestward Vanuatu
17 subduction zone (Fig. 1A).

18 Continental crust of north-eastern Zealandia underlies the Norfolk and Loyalty
19 Ridges (e.g., Schellart et al. 2006; Mortimer et al. 2017; Collot et al., 2020). These ridges
20 lie at c. 1000-1500 water depths and contrast with the back-arc basin oceanic crust of
21 the South Fiji and Norfolk basins which lies at 3000-4000 m water depth (Fig. 1). The
22 Loyalty and Three Kings Ridges are inferred to be the site of Cenozoic arc volcanism
23 (Crawford et al., 2003; Schellart et al., 2006; Maurizot et al., 2020a). However, only a few
24 rock samples have been recovered from these ridges in reconnaissance (Mortimer et al.
25 1998, 2007 2018) so their origin and nature are open to debate. Uncertainty about the
26 nature and age of the Loyalty and Three Kings Ridges results in first order ambiguities
27 concerning tectonic models of the geological evolution of the Cenozoic southwest Pacific

28 and, especially, the number, longevity, location and polarity of subduction zones (see
29 review by Collot et al., 2020).

30 The present study was designed to obtain volcanic rock samples from the
31 Loyalty and Three Kings ridges in order to fill SW Pacific geology's largest knowledge
32 gap. By retrieving and analyzing a large number of samples, our aim was to ground truth
33 the age range and polarity of subduction, and hence try to reconcile and test the variety
34 of Paleogene southwest Pacific tectonic models. In May-June 2015 the VESPA (Volcanic
35 Evolution of South Pacific Arcs) cruise of R/V *l'Atalante*, surveyed and dredged rocks
36 from along the Norfolk, Loyalty and Three Kings ridges and their adjacent basins
37 (Mortimer and Patriat, 2016). In total, useful igneous and sedimentary rock samples
38 were obtained from 36 out of 43 dredge sites (Fig. 1B). In this paper, we present
39 geochemical and isotopic data from the igneous rocks (mainly lavas) in order to : (1)
40 document the petrologic nature of volcanism on the Loyalty and Three Kings ridges; (2)
41 explore upper mantle composition and dynamics under this region; (3) use this
42 information to test models of the subduction history and more generally the
43 geodynamics of the SW Pacific during the Cenozoic.

44 This paper follows on from earlier reconnaissance petrology and dating studies
45 of pre-Quaternary SW Pacific dredge and onland samples (Mortimer et al., 1998, 2007,
46 2014, 2018; Bernardel et al., 2002; Meffre et al., 2002; Booden et al. 2011; Timm et al.,
47 2019). It is a companion paper to other outputs from the VESPA cruise (Patriat et al.,
48 2018; Gans et al., 2022, submitted; Collot et al., in preparation).

49

50 **2. Geological setting**

51

52 The entire study area of the Three Kings and Loyalty ridges is underwater. The closest
53 parts of Zealandia that are above sea level are New Caledonia and New Zealand. Despite
54 being 1500 km apart, these countries have several continental geological features in

55 common. These include thick crust, a basement of pre-Late Cretaceous accreted
56 terranes, Late Cretaceous to Miocene terrigenous-calcareous sedimentary basins, and
57 ophiolitic and sedimentary allochthons emplaced as northeast-verging nappes (Isaac et
58 al., 1994; Maurizot et al., 2020b). Some notable differences are (1) New Caledonia has
59 only a sparse record of arc magmatism in the form of Eocene dikes and two small
60 Oligocene plutons but northern New Zealand has several well-developed Early Miocene
61 to Holocene subduction-related volcanic-plutonic arc systems; (2) New Caledonia has a
62 Paleogene blueschist-eclogite facies metamorphic core whereas New Zealand lacks high
63 pressure metamorphic rocks; (3) the mantle-derived Peridotite Nappe of New Caledonia
64 was emplaced between c. 34 and 27 Ma. In contrast, the Northland Allochthon was
65 emplaced at 22-25 Ma and is dominated by a metavolcanic thrust sheet (Isaac et al.,
66 1994; Maurizot et al., 2020b).

67 Zealandia, along with Australia and Antarctica, was formerly part of the
68 southern supercontinent of Gondwana. Subduction-related magmatism persisted along
69 Gondwana's Pacific-facing margin until at least 110 Ma after which it started to separate
70 from Gondwana (Mortimer et al., 2017).

71 Sometime in the Paleocene or Eocene, a renewed episode of subduction is
72 thought to have commenced (Cluzel et al., 2006; 2012; ; Maurizot et al., 2020c).
73 Numerous alternative geodynamic models have been proposed to explain the initiation
74 and development of this younger SW Pacific subduction (see Matthews et al., 2015;
75 Collot et al., 2020 for reviews). As outlined above, the Loyalty and Three Kings ridges
76 are inferred to be remnant arcs of this older Paleogene subduction. Eocene arc lavas are
77 also found in Tonga and Fiji (Bloomer et al., 1995, , Meffre et al., 2012). The two ridges
78 are interpreted to have once been co-linear, having subsequently been separated by the
79 c. 400 km sinistral strike slip fault called the Cook Fracture Zone (Sdrolias et al., 2004;
80 Herzer et al., 2011). Using the orientation of the present-day Loyalty and Three Kings
81 ridges as a reference, one class of SW Pacific tectonic models proposes that an east-

82 dipping subduction zone initiated sometime in the Paleocene to Early Eocene (e.g.
83 Crawford et al., 2003; Cluzel et al., 2001, 2006; Schellart et al., 2006; Whattam et al.,
84 2006; Schellart, 2007). Subduction became collision by the arrival of the Norfolk Ridge
85 in the trench in the Late Eocene, resulting in an arc-continent collision that culminated
86 in the obduction of the overriding forearc (see review by Maurizot et al., 2020a). The
87 transition in space and time of the subduction flip to the present-day west-dipping
88 Pacific slab subduction is not a focus of these models which mainly address events
89 associated with the emplacement of the New Caledonia Peridotite Nappe.

90 In a contrasting class of models, a west-dipping subduction initiated in the
91 Eocene beneath the Loyalty-Three Kings ridge, and evolved via episodic Pacific trench
92 retreat to the present-day Tonga-Kermadec subduction (e.g. Malpas et al., 1992;
93 Mortimer et al., 1998; 2007; Sutherland et al., 2010;). A commonality in both classes of
94 model is that the Norfolk Ridge is assumed to be the easternmost continental part of
95 Zealandia, and the Loyalty-Three Kings Ridge the position of a Paleogene volcanic arc.
96 An attempt to reconcile the contrasting tectonic models was presented by Herzer et al.
97 (2011) who invoked an older east-dipping slab that became truncated by the west-
98 dipping Pacific slab as a triple junction spreading center migrated south.

99 Samples from the submarine SW Pacific ridges and basins recovered prior to the
100 VESPA cruise have been insufficient to test between the two general classes of model.
101 Knowledge of the geology of the Loyalty and Three Kings Ridges is particularly
102 important in this regard but, instead, there is a large data gap. On the Three Kings Ridge,
103 Mortimer et al., (1998, 2007) recovered Late Oligocene and Early Miocene andesites and
104 shoshonites and Bernardel et al. (2002) reported a 37 Ma old boninite lava and
105 serpentinite.

106 The basement of the Loyalty Ridge is even more poorly sampled and its origin
107 and nature, while prominently mentioned in the literature are almost completely
108 unsupported by actual rock samples. The Loyalty Islands that emerge from the ridge are

109 essentially composed of Mio-Pleistocene uplifted carbonate reefs; two Late Miocene
110 basaltic intraplate intrusions are reported on Maré Island (Maurizot et al., 2020c and
111 references therein). Elsewhere along the ridge, several Oligocene-Miocene intraplate
112 basalts have been sampled (Monzier et al., 1989; Mortimer et al., 2014). Because of its
113 possible spatial link with the D'Entrecasteaux Ridge located far north, where Eocene
114 subduction-related lavas have been sampled (Baker et al., 1994; Mortimer et al., 2014),
115 and in order to match with the geological interpretation of the Grande Terre of New
116 Caledonia, the Loyalty Ridge is often considered as an Eocene arc (Cluzel et al., 2001,
117 Crawford et al., 2003, Schellart et al., 2006, Matthews et al., 2012 Maurizot et al. 2020c).
118 However, no Eocene arc lavas have ever been obtained.

119

120 **3. Sampling strategy**

121

122 In order to test the above SW Pacific tectonic models we focused the sampling effort of
123 the 2015 VESPA cruise on the topographic highs of the Loyalty and Three Kings ridges,
124 and the intervening Cook Fracture Zone and South Fiji Basin seafloor (Fig. 1). Based on
125 experience from past expeditions, we anticipated issues with blanketing sediments,
126 limestone caps and/or ferromanganese crusts. Therefore, prior to dredging, we made
127 shallow seismic profiles and multibeam bathymetry surveys across the area. Sampling
128 was deliberately made in a relatively dense (for the area) dredging grid over north-
129 south and east-west baselines. Additionally, we took advantage of the steep scarps of the
130 Cook Fracture Zone and Cagou Trough to sample deep into the deepest parts of the two
131 ridges (Fig. 1). The fracture zone and trough walls enabled targeted dredging over
132 ~2500 m vertical height difference. To maximise sample recovery, our dredge sites
133 were preferentially made on steep rocky slopes.

134

135 **4. Petrographic and geochemical results**

136

137 *4.1. Petrographic features and lava classification*

138

139 The dredged igneous rocks are mainly basalts, with lesser trachybasalts, basaltic
140 andesites, trachyandesites andesites, dacites, and one granite. Basalts range from
141 aphyric to sparsely olivine, plagioclase and clinopyroxene-phyric to occasionally
142 moderately plagioclase-phyric. The other lavas are generally plagioclase-phyric and
143 biotite is a prominent phenocryst in trachyandesites and dacites. Some basalts are
144 vesicular and have amygdaloidal infillings of zeolite, carbonate and phosphatic
145 sediment. Many samples with a formerly glassy groundmass show moderate to
146 extensive secondary alteration (seafloor weathering) to orange-brown clay minerals
147 (Fig. S6).

148 Wherever possible, only the freshest parts of dredge samples were analysed (see
149 supplementary File 1 for detail). Despite this, elevated loss on ignition (LOI) values (e.g.
150 up to >10 wt% for sample DR07Ci) are present in our dataset. As such, we are
151 circumspect in our geochemical interpretation and try and place more emphasis on
152 using concentrations and ratios of rare earth elements (REEs) and high field strength
153 elements (HFSEs) rather than large ion lithophile elements (LILEs). The least altered
154 samples (LOI < 4 wt%) were classified according to their position in a total alkali-silica
155 plot (Le Bas et al., 1986; Fig 2A). Their chemical compositions confirm the wide
156 petrographic range, and include alkaline and subalkaline suites (confirmed by variation
157 in relatively immobile element ratios e.g. Nb/Y; not shown).

158 One of the first things apparent from our entire dataset is that samples dredged
159 from the deeper parts of the area e.g. South Fiji Basin, Cook Fracture Zone (blue symbols
160 in all figures) are basaltic. In contrast, samples dredged from the shallower levels of the
161 Loyalty and Three Kings ridges (yellow symbols in all figures) are more petrologically
162 evolved and are typically andesitic or trachytic. This difference is also reflected in K₂O

163 and other LILE contents. In the deep basaltic lavas ($\text{SiO}_2 < 49$ wt%, $\text{MgO} \sim 7.4$) K_2O is
164 typically low at 0.1 wt%, they are low-K tholeiites. In the shallower, intermediate
165 composition lavas ($\text{SiO}_2 < 57$ wt%, MgO 1.1- 5.4 wt%), K_2O ranges as high as 7 wt% and
166 many are classed as high-K and shoshonitic in the SiO_2 vs K_2O diagram of Peccerillo and
167 Taylor (1976) (Fig.2B). Primary high K_2O contents of these dredged VESPA lavas are
168 supported by the presence of biotite phenocrysts (Fig. S6).

169

170 *4.2. Trace element concentrations*

171 Trace element concentrations are reported in table S1, and shown on the multi-
172 element diagrams in Fig. 3. Based on REE patterns (Fig. 3 A-C) at least three distinct
173 groups can be distinguished, here called depleted (Fig. 3A), transitional (Fig. 3B) and
174 enriched (Fig. 3C) according to their light to heavy REE ratios, with La/Sm ranging from
175 0.4 to 8.

176 The samples most depleted in light REEs are two basalts from VESPA dredge 39
177 (depth ~ 3900 m) in the Cook Fracture Zone (Fig. 1, 3A and blue symbols on all
178 geochemical diagrams). They have $\text{SiO}_2 \sim 48.5$ wt%, $\text{MgO} \sim 7$ wt%. They display REE
179 concentrations similar to those found in normal mid-ocean ridge basalts (N-MORBs)
180 with La contents similar to primitive mantle (McDonough and Sun, 1995) and Lu
181 concentrations of about 4x primitive mantle. Nevertheless, their HFSE concentrations
182 appear slightly low compared to REE contents with $\text{Nb/Yb} = 0.17-0.19$ and LILEs display
183 higher concentrations than in N-MORB (with, for instance, Ba/Yb ranging from 3.6 to
184 10.7) suggesting that these signature are more typical of back-arc basin basalts (BABB)
185 rather than typical open ocean N-MORBs (Pearce and Stern, 2006). However, most of
186 these indicators (e.g., Ba, Rb concentrations) can easily be affected by alteration and it is
187 in turn difficult to assess with certainty if these samples correspond to BABB or to
188 normal-MORB suites.

189 Most basalts and basaltic andesites display flat, undepleted REE patterns (Fig.
190 3B). These lavas have REE contents ranging from 3 to >10 times primitive mantle,
191 depending on extent of fractionation, but nonetheless have remarkably constant REE
192 relative abundances. In the context of our dataset, we refer to these as transitional
193 basalts, but do not use this term to imply any alkaline character (as shown in Fig. 2A
194 most of the lavas are subalkaline). Most of these basalts also have HFSE depletions and
195 LILE enrichments relative to other incompatible elements, features which are typical of
196 subduction related fluid enrichments and therefore of arc lavas, and/or continental-
197 crust-contaminated intraplate basalts (Li et al., 2015; Mortimer et al., 2018). The trace
198 element signatures in these lavas are very similar to those reported for samples FAUST2
199 D3, collected along the CFZ and analysed by Bernardel et al (2002) (see supplementary
200 figure S1). On a Th/Yb vs Nb/Yb diagram (Fig.3E) of Pearce (2008) all of these lavas lie
201 in the field of back-arc basalts (as delimited by Li et al, 2015). All samples with these
202 geochemical characteristics were dredged from 3300-4800 m water depth along the
203 Cook Fracture Zone scarp (Fig. 1).

204 Basaltic andesites, andesites, trachyandesites and trachytes dredged at shallow-
205 water depth have the most incompatible element enriched compositions (Fig. 3C). Their
206 REE contents range over an order of magnitude ($La = 10$ to $100\times$ chondrite) and are
207 characterized by strong enrichments in the most incompatible LREE compared to HREE
208 (La/Yb ranging from 3 to 16). As with the transitional samples in Fig 3B, this group of
209 enriched lavas display chemical characteristics typical of subduction processes, such as
210 HFSE depletions and LILE enrichments as well as similar HREE contents (Yb ranging
211 from 2-10x chondrite. The main difference between the trace element signatures of this
212 and the other groups of samples is in the degree of light REE enrichments relative to
213 intermediate and heavy REE concentrations, with La/Sm ranging from 1 and 3.1 for the
214 basalts (Fig. 3B) on the one hand, and from 2.3 to 4.9 for the more evolved samples (Fig.
215 3C). These differences in REE spectra slopes cannot readily be accounted for by crystal

216 fractionation of the basalts (which would lead to parallel patterns), but instead may
217 indicate different degrees of partial melting, a more incompatible element enriched
218 source (for the LREE enriched lavas), or a combination of both. On the Th/Yb vs Nb/Yb
219 diagram (Fig.3E) of Pearce (2008), these samples lie in the field of island arc basalts.

220

221 *4.3. Pb, Hf, Nd and Sr isotopes*

222 The Pb, Hf, Nd and Sr of the samples are reported in Table S1. The Pb isotope
223 ratios of our entire VESPA dataset cover a relatively restricted range, with $^{208}\text{Pb}/^{204}\text{Pb}$
224 ranging from 38 to 39.8, $^{207}\text{Pb}/^{204}\text{Pb}$ ranging from 15.51 to 15.64 and $^{206}\text{Pb}/^{204}\text{Pb}$
225 ranging from 17.9 to 20.1. They plot systematically above the North Hemisphere
226 Reference Line of Hart (1984) on Fig. 4, so within typical Indian rather than Pacific
227 MORB fields (Crawford et al., 1995). Some possible mixing trends between end-
228 members can be seen in our dataset. In particular there seems to be an array between
229 depleted MORB mantle (DMM) and more enriched compositions (Fig. 5). The small
230 number of samples and limited range of compositions affect confidence in this trend.
231 Additionally there is another trend, mainly shown by the incompatible element enriched
232 lavas (yellow symbols on all figures) pointing towards an EM2 end-member (Hart et al.,
233 1992) (Fig. 5). A principal component analysis calculated on the Pb isotope data reveals
234 the existence of only two significant principal components (the first one accounting for
235 $\sim 76\%$ of the total variability, and the second for $\sim 23\%$, Fig. S3). This result affirms the
236 qualitative interpretation that the diversity of isotopic compositions observed in the
237 VESPA dataset can be accounted for by the mixing of no more than three components
238 along two arrays.

239 Hf isotopes range from typically depleted (N-MORB-like) signatures
240 ($^{176}\text{Hf}/^{177}\text{Hf}= 0.28317$, $\epsilon_{\text{Hf}}=+14$) to enriched (Ocean Island Basalt-like) compositions
241 ($^{176}\text{Hf}/^{177}\text{Hf}= 0.28299$, $\epsilon_{\text{Hf}}=+7.7$). The comparison of Hf isotopes with Pb isotopes (Figs.
242 4B, 5), reveals a sharper geochemical portrayal than Pb isotopes alone. A clear

243 distinction can be made between the depleted (DR39) and transitional groups on the
244 one hand and the enriched group on the other hand (Figs. 4Bis and 5).

245 The exact same features can be seen using Nd and Sr isotopes, although we note
246 the vulnerability of submarine basalts to weathering, despite the leaching in our sample
247 preparation. The VESPA lavas have $^{143}\text{Nd}/^{144}\text{Nd}=0.5128\text{-}0.5131$, $\epsilon_{\text{Nd}}= 2.8\text{-}9.3$ and
248 $^{87}\text{Sr}/^{86}\text{Sr}= 0.79026\text{-}0.7048$, both of which are correlated with Hf data (Fig. 5).

249

250 **5. Discussion**

251

252 *5.1 Mantle source compositions and conditions of melting*

253 The three distinct trace element signature groups recognized on Fig. 3 (depleted,
254 transitional and enriched in incompatible elements) can theoretically be accounted for
255 by different amounts of melting, fractionation, source compositions or a combination of
256 all three. Nevertheless, the wide range in trace element concentrations and ratios (e.g.
257 La/Sm ranging 0.3 to >8) makes it very unlikely that the parent melts of all samples
258 shared a common mantle source.

259 Both the depleted and the transitional tholeiitic basalt groups (blue symbols),
260 have HFSE depletions and LILE enrichments suggesting that these magmas were likely
261 produced by the decompression melting of the moderately fluid-enriched upper mantle,
262 which is a common feature of both back-arc basin basalts (BABBs) (e.g. Pearce and
263 Stern, 2006), forearc basalts (FABs) (e.g. Reagan et al., 2010; Falloon et al 2014), Fijian
264 early arc basalts (Todd et al. 2012) and SW Pacific rear-arc basalts from the Colville
265 Ridge (Timm et al. 2019). The main geochemical distinctions proposed for BABB and
266 FAB are based on the relative abundances of REE and vanadium; FABs typically feature
267 higher REE/V than BABBs. A wide overlap exists between these populations, and our
268 Loyalty-Three Kings tholeiites all lie within this broad compositional range
269 (Supplementary Fig. S.2.) but, overall, show more affinity with rear-arc and back-arc

270 basin basalts. The incompatible element-enriched group (yellow symbols) show a wide
271 range in normalised anhydrous SiO₂ (51-65 wt%), MgO (1-7 wt%)_and Cr (1-360 ppm)
272 but defy attempts to apply depth of melting geobarometers and interpretation via
273 simple modelling of melting and fractional crystallization processes. Clearly, their
274 chemistry is more typical of hydrous flux-melting products than the depleted and
275 transitional lavas (Fig. 3) and could therefore be accounted for by the building of an arc
276 at 25-22 Ma..

277 The variability and clustering of Pb, Hf, Nd and Sr isotopic compositions confirm
278 that different mantle sources melted to generate the depleted, transitional and enriched
279 lavas. One isotopic component overlaps those of Pacific and Indian N-MORB (grey and
280 green fields on Fig. 4 and 5) and can therefore be interpreted as normal depleted
281 ambient upper mantle. The two depleted BABB-like samples DR39A and B appear to be
282 the “purest” carriers of this signature (Fig. 5) and can be compared with approximately
283 coeval adjacent South Fiji Basin basalts (Todd et al. 2011). The trend defined by these
284 two samples together with all the transitional group possibly points toward more
285 enriched compositions (especially in Pb-Hf space), which, speculatively, could be the
286 second component of the mixture (the purple trend on Fig. 5). This tendency is a
287 relatively common feature of SW Pacific volcanic rocks (see for example the grey area
288 representing Pacific MORB on Fig.5) and is referred here as an “enriched-Pacific-MORB”
289 (EPM) component. It has, for instance, been well documented in intraplate,
290 intracontinental volcanism of Zealandia (e.g. Timm et al., 2010). The ubiquity of this
291 signature within the SW Pacific suggests that the DMM-EPM trend, also possibly shown
292 by our samples, probably reflects the melting of the naturally heterogeneous upper
293 mantle beneath the SW Pacific and Zealandia. The Miocene Northland Arc is anchored in
294 Zealandia continental crust and a wide variety of basalts, andesites, dacites and
295 rhyolites are reported from several volcanic centres (Isaac et al. 1994). Unfortunately,
296 only Sr and Nd isotopic data are available for these rocks (Booden et al., 2011) so they

297 are of limited use in characterising the Miocene continental mantle wedge under
298 Zealandia.

299 The third geochemical component revealed on Figures 4 and 5 (pink trend on
300 Fig. 5), has Pb isotopic compositions similar to those of the DMM-EPM mixture
301 described above (blue trend on Fig.5). It is therefore mostly defined using Sr, Hf and Nd
302 isotopes (Fig. 4 and 5) and is represented by the most geochemically enriched
303 (intermediate to felsic) samples, shown as yellow diamonds in all figures. Its
304 unradiogenic Hf and Nd, and its radiogenic Sr signatures can be interpreted in two
305 different ways. First, it could simply reflect the effect of crustal contamination on mantle
306 melts. This possibility is supported by a broad correlation existing between isotope
307 signatures and Ce/Pb and Nb/U ratios (Fig. S4), which are classic proxies for
308 continental crust contamination (Hofmann et al., 1986; Rudnick and Fountain, 1996).
309 Nevertheless, in samples defining the trend (pink band, yellow diamonds on Fig. 5),
310 cover the same range as most of those, featured by the basaltic samples belonging to the
311 previous trend (DMM-EPM, blue circles. purple band) and no clear correlation can be
312 established between isotopes and major elements such as SiO₂ and Al₂O₃. Moreover, if
313 Ce/Pb and Nb/U are particularly low in continental crust material (Rudnick and
314 Fountain, 1995) compared to MORB (Gale et al., 2015), they can be just as low in arc
315 related melts, as illustrated in Fig. S5 (Gale et al. 2015; Turner and Langmuir, 2015; Yang
316 et al., 2021). It is in turn difficult to assert that these geochemical signatures are strictly
317 due to crustal contamination. In any case, the continental crust under the TKR and LR is
318 likely to be relatively young (Jurassic to Cretaceous) and relatively low ⁸⁷Sr/⁸⁶Sr, and
319 high bulk ¹⁴³Nd/¹⁴⁴Nd, as such reported for the Waipapa Terrane accretionary wedge
320 (Adams and Maas, 2004). Therefore, the signal of such contamination would be subtle.
321 The second simple explanation, for the pink band EM2 isotopic trend, would be the
322 addition of variable amounts of subducted sediments to the mantle wedge, as has been
323 documented for other subduction zones worldwide and in the SW Pacific by Timm et al.

324 (2019) and Mortimer et al. (2022).

325

326 *5.3 Chronology*

327 On Fig. 6, crystallization ages are compared with geography, Hf isotopes and
328 La/Sm ratios in order to explore across-arc trends, involvement of mantle sources and
329 degree of geochemical enrichment with time. The vast majority of sampled and dated
330 lavas from the Loyalty and Three Kings ridges fall in a relatively narrow range of ~25 to
331 ~22 Ma i.e. latest Oligocene to earliest Miocene. The age range of the three different
332 geochemical groups overlap with depleted basalts ~23 and ~22 Ma, transitional basalts
333 ~25 to 22 Ma, and enriched lavas ~25 to 22 Ma. Thus, there is no clear geochemical
334 change with age, nor with east-west distance (Fig. 6). However, as previously noted,
335 there is a geochemical change with current water depth, with depleted and intermediate
336 basalts occurring at deep levels and enriched lavas at shallow levels. The overlapping
337 ages do not necessarily refute a crude correspondence of water depth with stratigraphy
338 but attest to the rapidity of build-up of the volcanic piles and operation of different
339 petrogenetic processes in the short 25 to ~22 Ma time interval.

340 Two tholeiitic basalts in our dataset (VESPA DR25A and DR25C), collected
341 within a single dredge at 3850 meters deep along the east side of the Cagou Trough,
342 stand out as being substantially older than 25-21 Ma. Despite being dated at 36 and 38
343 Ma, these DR25 basalts are geochemically indistinguishable from the more numerous
344 25-21 Ma transitional basalts.

345

346 *5.3 Geodynamic interpretation*

347 Our study area of the Loyalty and Three Kings ridges is approximately halfway
348 between New Caledonia and New Zealand. As such our geochemical results provide

349 useful ground truthing and have several important implications for the tectonic
350 development of the SW Pacific region (Fig. 7). The main interpretations that can be
351 made are: Documentation of a major pulse of subduction-related magmatism that has
352 built up the arcs of the Loyalty and Three Kings ridges in the Late Oligocene to Early
353 Miocene. This confirms the formerly-joined ridges as a single volcanic arc and is at odds
354 with existing geodynamic models which assumed the subduction zone and arc were far
355 to the east in Early Miocene (e.g. Crawford et al., 2003; Schellart et al., 2006; Whattam et
356 al., 2006; Meffre et al., 2012). Late Oligocene-Early Miocene arc volcanism, previously
357 documented on the Three Kings Ridge (Mortimer et al., 1998, 2007) is now shown to be
358 present on the Loyalty Ridge and so must be incorporated into the post-obduction
359 history of New Caledonia.

360 The Loyalty-Three Kings ridge lavas are dominated by basalts. Geochemically,
361 compositions overlap with reference suites of back-arc basin basalts and low-K arc
362 tholeiites. Our extensive vertical and lateral sampling from the crests to the bases of the
363 Loyalty and Three Kings ridges, documents the major presence of subducted-related
364 basalts. Basaltic andesites and andesites are rare (and rhyolite is absent) in our data set
365 whereas these are relatively common rock types in other volcanic arcs. It is difficult to
366 unambiguously assign an independent tectonic setting of eruption to the Loyalty-Three
367 Kings basalts on a sample-by-sample geochemical basis but, overall, an arc setting is
368 preferred because of the buildup of a linear volcanic ridge. The Cook Fracture Zone may
369 represent a 'leaky transform' style of volcanism in a disrupted arc setting akin to that on
370 the Northland Plateau (Mortimer et al., 2007). Trachyandesites and trachytes are
371 exposed on the topmost crests of the Loyalty-Three Kings Ridge. They show shoshonitic
372 affinities.

373 The across-strike width of co-eval subduction-related volcanism is possibly
374 wider in the Loyalty-Three Kings Ridge than in other SW Pacific arcs such as the Lau-
375 Colville and Tonga-Kermadec ridge systems. In part this may be due to more broad or

376 diffuse volcanism expected at a continental margin, and in part due to syn- or post-
377 magmatic extension e.g. in the Cagou Trough and Kwênyii Basin (Mortimer et al., 2007,
378 2020c; Patriat et al., 2018). Two granite plutons in New Caledonia of 24 and 27 Ma age
379 (Cluzel et al., 2005; Paquette and Cluzel, 2007) display geochemical characteristics
380 similar to our EM2 trend lavas (towards EM-2). It is therefore possible that they are
381 petrogenetically related.

382 Four pre-Late Oligocene subduction-related volcanic rocks have now been
383 dredged from the Three Kings Ridge and range in age from ~38-32 Ma (Bernardel et al.,
384 2002; Mortimer et al., 2007; this study). These pre-Late Oligocene lavas represent a very
385 small minority in our data set and they have all been recovered on the westernmost side
386 of the Three Kings Ridge. Rocks of this age may reasonably be inferred to be also present
387 on the westernmost edge of the Loyalty ridge, i.e. on the Félicité Ridge. However, the
388 only area along the strike of the Loyalty arc where Eocene rocks have been recovered
389 and dated is the D'Entrecasteaux Ridge, some 1000 km NW of our study area (Baker et
390 al., 1994; Mortimer et al., 2014).

391 Mantle sources for the Loyalty-Three Kings arc lavas were heterogeneous. Lavas
392 lie on trends between DMM, an “enriched-Pacific-MORB” and a EM2-like component.
393 This is an expected mix of mantle types in the SW Pacific oceanic region adjacent to the
394 Zealandia continent. Together with the Indian/Gondwana nature of the DMM
395 component and EM-2 / Zealandia continental component, it may provide tentative
396 evidence for persistent west-dipping subduction, occurring in Oligocene-Miocene time
397 under the Loyalty-Three Kings ridge, before retreating under the Lau-Colville, and
398 Tonga-Kermadec ridges.

399 Collectively, these new constraints lead us to propose a revised tectono-
400 petrogenetic evolution model of the SW Pacific as shown in Figure 7: the Eocene
401 subduction, initiated around 56 Ma, ended with the obduction of the Peridotite Nappe in
402 New Caledonia during the Late Eocene-Early Oligocene (Cluzel et al., 2001; Maurizot et

403 al., 2020a). We cannot comment with any confidence about the subduction polarity of
404 this Eocene subduction because lavas of this age are rare. But in our view, all the
405 Paleogene magmatism within the Poya Terrane (including our DR25 samples), plausibly
406 fits as BABB, or FAB related to a west-dipping subduction along the eastern edge of
407 Zealandia. Accordingly, Figure 7A shows the end of the Eocene subduction stage with a
408 west-dipping slab, which is in agreement with the long duration of the Paleogene
409 magmatic activity within the Poya Terrane (more than 10 My, Cluzel et al., 2017 and
410 references therein) and a flake tectonic interpretation of ophiolite obduction (Malpas et
411 al. 1992). Nevertheless, subduction flips during this time interval are also viable.
412 Whatever the polarity, an important new information brought by our study is that the
413 main magmatic phase attesting of the building of an arc along the LR and TKR happened
414 after this stage of obduction and is therefore clearly distinct from the Eocene
415 subduction.

416 Obduction was followed by a period of post-orogenic extension (Lagabrielle et
417 al., 2005; Patriat et al., 2018) accompanied by sparse magmatism as indicated by the 32
418 Ma Early Oligocene lava on Three Kings Ridge (Mortimer et al., 2007), the New
419 Caledonia granites (Cluzel et al., 2005; Paquette et al., 2007) and the Northland supra-
420 subduction zone ophiolites of this age (Whattam et al., 2006). These scattered suites are
421 related in time but not necessarily in petrogenesis. At this time, the supra subduction
422 margin was composed of an obducted oceanic lithosphere stretched and fractured by
423 normal faults (Patriat et al., 2018) lying over the similarly stretched and thinned eastern
424 continental margin of Zealandia (Fig. 7B).

425 At around 25 Ma, thick piles of lava of different compositions erupted in and
426 around the LR and TKR (Fig. 7C). A variety of igneous processes operated. Subduction at
427 the eastern edge of the Zealandian thinned margin induced a phase of decompression
428 melting of the normal Pacific upper mantle (our so-called transitional lavas and an
429 isotopic DMM-EPM trend). Simultaneously, steepening of the slab accompanied its

430 eastward rollback, and induced a significant increase of the slab derived fluid into the
431 wedge, leading to the generation of magmas from EM2-like geochemically enriched
432 material (our so-called enriched lavas and isotopic trend towards EM2). This flux
433 melting led to the eruption of what are now the shallow water parts of the Loyalty and
434 Three Kings ridges. Steepening of the slab and increase of the slab derived fluid input
435 into the wedge explains the shoshonitic compositions as are observed e.g. in the Aeolian
436 arc (Morrison, 1980). Alternatively and/or additionally, the shoshonites can also be
437 related to rollback-related extension of the arc (Mortimer et al. 2007, 2022).

438 After migration of arc-related volcanism away from LR and TKR, the eastward
439 roll-back of the Pacific slab and associated trench retreat, accelerated (Fig. 7D). This
440 may have induced further extension in New Caledonia in the Miocene (e.g. Sevin et al.
441 2020). The decompression melting of the depleted DR39 BABBs may have taken place at
442 this time, along with rapid generation of oceanic crust in the Norfolk and South Fiji
443 basins, accompanied by sinistral movement on the Cook Fracture Zone (Herzer et al.,
444 2011). The arc later stabilised further east, along the Lau-Colville Ridge (Timm et al.,
445 2019) and, subsequently, the Tonga-Kermadec Ridge.

446

447 **6. Conclusions**

448 Results of new analyses of lava samples collected along and across the Three Kings
449 and Loyalty ridges during the 2015 VESPA expedition provide a unique and informative
450 geochemical-space-time perspective on the magmatic and tectonic evolution of the SW
451 Pacific. Almost all dredged lavas are subduction-related and erupted between 25 and 22
452 Ma, although two lavas are of ~ 38-36 Ma age. Their trace element and isotopic
453 compositions can be explained in terms of three distinct geochemical end-members in
454 the mantle sources (DMM, enriched-Pacific-MORB and EM-2 like) and two different
455 melting processes (decompression melting producing tholeiitic magmas and flux
456 melting producing high-K magmas).

457 The main conclusions arising from this study of SW Pacific lavas is that subduction-
458 related magmatism is confirmed on the Loyalty Ridge and this observation must be
459 incorporated into tectonic models of New Caledonia obduction. There is a strong
460 correlation between geochemical grouping and present-day water depth, with low-K
461 tholeiitic basalts dredged in deep water and high-K to shoshonitic lavas from shallower
462 ridge crests. The Loyalty-Three Kings arc was most active in the Late Oligocene to Early
463 Miocene. The issue of polarity of subduction remains open, but the composition and
464 distribution of the VESPA igneous rocks can be explained using a west-dipping
465 subduction model since Eocene time.

466

467 **Data Availability Statement**

468 Supplementary data files that support the findings of this study are openly available
469 <https://www.seanoe.org/data/00789/90050/>. General information about the VESPA
470 cruise can be found in the SISMER repository at <http://doi.org/10.17600/15001100>.

471

472 **Acknowledgements**

473 We thank the captain and crew of R/V l'Atalante and our onboard colleagues Claire
474 Bassoullet, Hamish Campbell, Mederic Amann, Nina Jordan, Charline Guerin, Caroline
475 Juan, Mathieu Mengin, Mathilde Pitel, Clement Roussel and Fanny Soetaert for their
476 support during the VESPA cruise. Agranier is particularly grateful to Claire Bassoullet
477 for her help before and during the VESPA cruise. The VESPA cruise was funded by the
478 Commission Nationale Flotte Hauturière of the French Ministry of Research and Higher
479 Education, with support from the governments of New Zealand and New Caledonia. We
480 acknowledge l'Institut National des Sciences de l'Univers, CNRS- Institut des Sciences de
481 la Terre, LabEx Mer, Service Géologique de Nouvelle Calédonie and the New Zealand
482 Ministry of Business, Innovation and Employment for post-cruise financial support. The
483 manuscript was improved by comments from two anonymous reviewers.

484

485 **References**

- 486 Adams C.J. & Maas R., 2004. Age/isotopic characterisation of the Waipapa Group in
487 Northland and Auckland, New Zealand, and implications for the status of the
488 Waipapa Terrane, New Zealand Journal of Geology and Geophysics, 47:2, 173-187,
489 DOI: 10.1080/00288306.2004.9515046
- 490 Agranier, A., Maury, R.C. , Geoffroy, L. , Chauvet, F. , Le Gall, B. , Viana, A.R., 2019. Volcanic
491 record of continental thinning in Baffin Bay margins: insights from Svartenhuk
492 Halvo Peninsula basalts, West Greenland. Lithos 334-335, 117–140.
- 493 Baker, P.E., Coltorti, M., Briquieu, L., Hasenaka, T., Condliffe, E., Crawford, A.J., 1994.
494 Petrology and composition of the volcanic basement of Bougainville Guyot, site
495 831. Proceedings of the Ocean Drilling Program Scientific Results 134, 363–373.
- 496 Bernardel, G., Carson, L., Meffre, S., Symonds, P., Mauffret, A., 2002. Geological and
497 morphological framework of the Norfolk Ridge to Three Kings Ridge region,
498 Geoscience Australia Record,2002/08.
- 499 Blichert-Toft, J., Chauvel, C., Albarede, F., 1997. Separation of Hf and Lu for high-
500 precision isotope analysis of rock samples by magnetic sector multiple collector
501 ICP-MS. Contributions to Mineralogy and Petrology 127, 248–260.
- 502 Blichert-Toft, J., Agranier, A., Andres, M., Kingsley, R., Schilling, J., Albarède, F., 2005.
503 Geochemical segmentation of the Mid-Atlantic Ridge north of Iceland and ridge-
504 hot spot interaction in the North Atlantic. Geochemistry Geophysics Geosystems 6.
505 <https://doi.org/10.1029/2004GC000788>
- 506 Bloomer, S. H., Taylor, B. , MacLeod, C. J. , Stern, R. J. , Fryer, P. , Hawkins, J. W., and
507 Johnson, L., 1995. Early arc volcanism and the ophiolite problem: A perspective
508 from drilling in the western Pacific, in *Active Margins and Marginal Basins of the*
509 *western, in Pacific Geophysical Monograph Series*, edited by B. Taylor et J. Natlan,
510 pp. 1-30, AGU, Washington D.C.

511 Booden, M.A., Smith, I.E.M., Black, P.M., Mauk, J.L., 2011. Geochemistry of the Early
512 Miocene volcanic succession of Northland, New Zealand, and implications for the
513 evolution of subduction in the Southwest Pacific. *Journal of Volcanology and*
514 *Geothermal Research* 199, 25–37.


515 Chauvel, C., Hofmann, A.W. and Vidal, P., 1992. HIMU-EM: the French Polynesian
516 connection. *Earth and Planetary Science Letters* 110, 99–119.

517 Cluzel, D., Aitchison, J.C., Picard, C., 2001. Tectonic accretion and underplating of mafic
518 terranes in the Late Eocene intraoceanic fore-arc of New Caledonia (Southwest
519 Pacific): geodynamic implications. *Tectonophysics* 340, 23–59.

520 Cluzel, D., Bosch, D., Paquette, J.L., Lemennicier, Y., Montjoie, P., Ménot, R.P., 2005. Late
521 Oligocene post-obduction granitoids of New Caledonia: A case for reactivated
522 subduction and slab break-off. *Island Arc* 14, 254–271.

523 Cluzel, D., Meffre, S., Maurizot, P., Crawford, A.J., 2006. Earliest Eocene (53 Ma)
524 convergence in the Southwest Pacific: Evidence from pre-obduction dikes in the
525 ophiolite of New Caledonia. *Terra Nova* 18, 395–402.

526 Cluzel, D., F. Jourdan, S. Meffre, P. Maurizot, and S. Lesimple, 2012. The metamorphic
527 sole of New Caledonia ophiolite: $^{40}\text{Ar}/^{39}\text{Ar}$, U-Pb, and geochemical evidence for
528 subduction inception at a spreading ridge, *Tectonics*, 31(3), doi:
529 10.1029/2011tc003085.

530 Cluzel, D., Whitten, M., Meffre, S., Aitchison, J. C., Maurizot, P., 2017. A reappraisal of the
531 Poya Terrane (New Caledonia): Accreted Late Cretaceous- Paleocene marginal
532 basin upper crust, passive margin sediments, and early Eocene E-MORB sill
533 complex. *Tectonics* 36. <https://doi.org/10.1002/2017TC004579> 

534 Collot, J., Patriat, M., Sutherland, R., Williams, S., Cluzel, D., Seton, M., Pelletier, B., Roest,
535 W.R., Etienne, S., Bordenave, A., Maurizot, P., 2020. Geodynamics of the SW Pacific:
536 a brief review and relations with New Caledonian geology. p 13–26 in Maurizot, P.,

537 Mortimer, N. (editors). New Caledonia: geology, geodynamic evolution and
538 mineral resources. Geological Society, London, Memoir 51.

539 Cotten, J., Le Dez, A., Bau, M., Caroff, M., Maury, R., Dulski, P., Fourcade, S., Bohn, M.,
540 Brousse, R., 1995. Origin of anomalous rare-earth element and yttrium
541 enrichments in subaerially exposed basalts, evidence from French Polynesia.
542 *Chemical Geology* 119, 115–138.

543 Crawford, A.J., Briquieu, L., Laporte, C., Hasenaka, T., 1995. Coexistence of Indian and
544 Pacific oceanic upper mantle reservoirs beneath the central New Hebrides island
545 arc. *Geophysical Monograph* 88, 199–217.

546 Crawford, A.J., Meffre, S., Symonds, P.A., 2003. 120 to 0 Ma tectonic evolution of the
547 south- west Pacific and analogous geologic evolution of the 600 to 220 Ma Tasman
548 Fold Belt System. *Geological Society of Australia Special Publication* 22, 377–397.

549 Douglas, J., Schilling, J.G., 2000. Systematics of three-component, pseudo-binary mixing
550 lines in 2D isotope ratio space representations and implications for mantle
551 plume–ridge interaction. *Chemical Geology* 163. 1–23

552 Falloon, T.J., Meffre, S., Crawford, A.J., Hoernle, K., Hauff, F., Bloomer, S.H., Wright, D.J.,
553 2014. Cretaceous fore-arc basalts from the Tonga arc: Geochemistry and
554 implications for the tectonic history of the SW Pacific. *Tectonophysics* 630, 21–32.

555 Fietzke, J., Eisenhauer, A., 2006. Determination of temperature-dependent stable
556 strontium isotope (Sr-88/Sr-86) fractionation via bracketing standard MC-ICP-
557 MS. *Geochemistry Geophysics Geosystems* 7, Q08009.

558 Gale, A., Dalton, C. A., Langmuir, C. H., Su, Y. & Schilling, J.-G. (2013), The mean
559 composition of ocean ridge basalts. *Geochem. Geophys. Geosyst.* **14**, 489–518.

560 Gans, P.B., Mortimer, N. , Patriat, M. , Turnbull, R.E. , Crundwell, M. , Agranier, A. , Calvert,
561 A., Seward, G., Etienne, S., Durance, P. M. , Campbell, H.J. , Collot, J.,
562 2022. Argon/Argon, micropaleontological and Uranium/Lead geochronological

563 data for igneous and sedimentary rocks dredged during the VESPA scientific
564 cruise. SEANOE. <https://doi.org/10.17882/89740>

565 Gans, P.B., Mortimer, N., Patriat, M., Turnbull, R.E., Crundwell, M.P., Agranier, A., Calvert,
566 A.C., Seward, G., Etienne, S., Durance, P.M.J., Campbell, H.J., Collot, J. Detailed
567 $^{40}\text{Ar}/^{39}\text{Ar}$ geochronology of the Loyalty and Three Kings Ridges clarifies the extent
568 and sequential development of Eocene to Miocene southwest Pacific remnant
569 volcanic arcs. Submitted to *Geochem. Geophys. Geosyst.*

570 Hart, S.R., 1984. A large scale isotope anomaly in the Southern Hemisphere mantle,
571 *Nature* 309, 753– 757.

572 Hart, S.R., Hauri, E.H., Oschmann, L.A., Whitehead, J.A. 1992. Mantle plumes and
573 entrainment - isotopic evidence. *Science* 256, 517–520.

574 Herzer, R.H., Barker, D.H.N, Roest, W.R., Mortimer, N., 2011. Oligocene-Miocene
575 spreading history of the northern South Fiji Basin and implications for the
576 evolution of the New Zealand plate boundary. *Geochemistry Geophysics*
577 *Geosystems* 12, Q02004. <http://doi.org/10.1029/2010GC003291>.

578 Isaac, M.J., Herzer, R.H., Brook, F.J., Hayward, B.W., 1994. Cretaceous and Cenozoic
579 sedimentary basins of Northland, New Zealand. *Institute of Geological and Nuclear*
580 *Sciences Monograph* 8, 230 pp.

581 Le Bas, M.J., Le Maitre, R.W., Streckeisen, A., Zanettin, B., 1986. A chemical classification
582 of volcanic rocks based on the total alkali silica diagram. *Journal of Petrology* 27,
583 745–750.

584 Li, Z.x.A., Lee, C.T.A., 2006. Geochemical investigation of serpentized oceanic
585 lithospheric mantle in the Feather River Ophiolite, California: Implications for the
586 recycling rate of water by subduction. *Chemical Geology* 235, 161-185.

587 Li, C., Arndt, N.T., Tang, Q., Ripley, E.M., 2015. Trace element indiscrimination diagrams.
588 *Lithos* 232, 76–83.

589 Malpas, J., Sporli, K.B., Black, P.M., Smith, I.E.M., 1992. Northland ophiolite, New Zealand,
590 and implications for plate-tectonic evolution of the southwest Pacific. *Geology* 20,
591 149–152.

592 Matthews, K.J., Williams, S.E., Whittaker, J.M., Müller, D., Seton, M., Clarke, G.L., 2015.
593 Geologic and kinematic constraints on Late Cretaceous to mid Eocene plate
594 boundaries in the southwest Pacific. *Earth-Science Reviews* 140, 72–107.

595 Maurizot, P., Cluzel, D., Patriat, M., Collot, J., Iseppi, M., Lesimple, S., Secchiari, A., Bosch,
596 D., Montanini, A., Macera, P., Davies, H.L., 2020a. The Eocene Subduction–
597 Obduction Complex. p 93–130 in Maurizot, P., Mortimer, N. (editors). *New*
598 *Caledonia: geology, geodynamic evolution and mineral resources*. Geological
599 Society, London, Memoir 51.

600 Maurizot, P., Robineau, B., Vendé-Leclerc, M., Cluzel, D., 2020b. Introduction. p 1–14 in
601 Maurizot, P., Mortimer, N. (editors). *New Caledonia: geology, geodynamic*
602 *evolution and mineral resources*. Geological Society, London, Memoir 51.

603 Maurizot, P., Collot, J., Cluzel, D., Patriat, M., 2020c. The Loyalty Islands and Ridge, New
604 Caledonia. p 131–145 in Maurizot, P., Mortimer, N. (editors). *New Caledonia:*
605 *geology, geodynamic evolution and mineral resources*. Geological Society, London,
606 Memoir 51.

607 McDonough, W.F., Sun, S.S., 1995. The composition of the Earth. *Chemical Geology* 120,
608 223–253.

609 Meffre, S., Symonds, P., Bernardel, G., Carson, L., Crawford, A.J., 2002. Oligocene collision
610 of the Three Kings Ridge and initiation of the Tonga–Kermadec island arc system.
611 *Western Pacific Geophysics Meeting Supplement*, abstract SE41D-07. *Eos*,
612 *Transactions American Geophysical Union* 83 (22), 91–92.

613 Meffre, S., Falloon, T.J., Crawford, A.J., Hoernle, K., Hauff, F., Duncan, R.A., Bloomer, S.H.
614 Wright, D. J., 2012. Basalts erupted along the Tongan fore arc during subduction
615 initiation: Evidence from geochronology of dredged rocks from the Tonga fore arc

616 and trench, *Geochemistry Geophysics Geosystems* 13, Q12003,
617 doi:10.1029/2012GC004335.

618 Monzier, M., Boulin, J., Collot, J.-Y., Daniel, J., Lallemand, S., Pelletier, B., 1989. Premiers
619 résultats des plongées Nautille de la campagne SUBPSO-I sur la zone de collision a
620 ride des Loyauté arc des Nouvelles-Hébrides (Sud-Ouest Pacifique). *Comptes*
621 *Rendu Academie des Sciences Paris Serie 2*(309), 2069–2076.

622 Morrison, G.W., 1980. Characteristics and tectonic setting of the shoshonite rock
623 association. *Lithos* 13, 97–108.

624 Mortimer, N., Patriat, M., 2016. VESPA cruise report. Volcanic Evolution of South Pacific
625 Arcs. n/o L'Atalante, Nouméa – Nouméa, 22 May-17 June 2015. SGNC Rapport N°
626 SGNC – 2016 (02). Retrieved from <http://archimer.ifremer.fr/doc/00343/45408/>

627 Mortimer, N., Herzer, R.H., Gans, P.B., Parkinson, D.L., Seward, D., 1998. Basement
628 geology from Three Kings Ridge to West Norfolk Ridge, southwest Pacific Ocean:
629 evidence from petrology, geochemistry and isotopic dating of dredge samples.
630 *Marine Geology* 148, 135–162.

631 Mortimer, N., Campbell, H. J., Tulloch, A.J., King, P.R., Stagpoole, V.M., Wood, R.A.,
632 Rattenbury, M.S., Sutherland, R., Adams, C.J., Collot, J., Seton, M. , 2017. Zealandia:
633 Earth's hidden continent. *GSA Today*, 27(3), 28–35.

634 Mortimer, N., Herzer, R.H., Gans, P.B., Laporte-Magoni, C., Calvert, A.T., Bosch, D., 2007.
635 Oligocene–Miocene tectonic evolution of the South Fiji Basin and Northland
636 Plateau, SW Pacific Ocean: evidence from petrology and dating of dredged rocks.
637 *Marine Geology* 237, 1–24.

638 Mortimer, N., Gans, P.B., Palin, J.M., Herzer, R.H., Pelletier, B., Monzier, M., 2014. Eocene
639 and Oligocene basins and ridges of the Coral Sea-New Caledonia region: tectonic
640 link between Melanesia, Fiji, and Zealandia. *Tectonics* 33, 1386–1407.

641 Mortimer, N., Gans, P.B., Meffre, S., Martin, C.E., Seton, M., Williams, S., ... Rollet, N. 2018.
642 Regional volcanism of northern Zealandia: post-Gondwana breakup magmatism

643 on an extended, submerged continent. Geological Society, London, Special
644 Publication 463, 199–226.

645 Mortimer, N., Patriat, M., Gans, P.B., Agranier, A., Chazot, G., Collot, J., Crundwell, M.P.,
646 Durance, P.M.J., Campbell, H.J., Etienne, S., 2021. The Norfolk Ridge seamounts:
647 Eocene-Miocene volcanoes near Zealandia's rifted continental margin. Australian
648 Journal of Earth Sciences 68, 368–380.

649 Mortimer, N., Gans, P.B., Turnbull, R.E., Patriat, M., Agranier, A., Durance, P.M.J., Etienne,
650 S., Campbell, H.J., Chazot, G., Crundwell, M.P., Hollis, C.J., Collot, J. 2020b. Volcanism
651 between New Zealand and New Caledonia: a stretched Late Eocene to Early
652 Miocene magmatic arc on the Loyalty and Three Kings Ridges. Geoscience Society
653 of New Zealand Annual Conference Abstract, Nov. 2020. Geoscience Society of
654 New Zealand Miscellaneous Publication 157A, 191.

655 Mortimer, N., Bosch, D., Laporte-Magoni, C., Todd, E., Gill, J.B. 2022. Sr, Nd, Hf and Pb
656 isotope geochemistry of Early Miocene shoshonitic lavas from the South Fiji Basin:
657 note. New Zealand Journal of Geology and Geophysics, in press.
658 <https://doi.org/10.1080/00288306.2021.1876110>

659 Mougél, B., Agranier, A., Hemond, C., Gente, P., 2014. A highly unradiogenic lead isotopic
660 signature revealed by volcanic rocks from the East Pacific Rise. Nature
661 Communications 5, 4474. <https://doi.org/10.1038/ncomms5474>

662 Moynier, F., Agranier, A., Hezel, D.C., Bouvier, A., 2010. Sr stable isotope composition of
663 Earth, the Moon, Mars, Vesta and meteorites. Earth and Planetary Science Letters
664 300, 359–366.

665 Patriat, M., Collot, J., Etienne, S., Poli, S., Clerc, C., Mortimer, N., Pattier, F., Juan, C., Roest,
666 W. and VESPA scientific voyage team, 2018. New Caledonia obducted peridotite
667 nappe: offshore extent and implications for obduction and postobduction
668 processes. Tectonics 37, 1077–1096.

669 Paquette J.-L., Cluzel, D., 2007. U-Pb zircon dating of post-obduction volcanic-arc
670 granitoids and a granulite-facies xenolith from New Caledonia: inference on
671 Southwest Pacific geodynamic models. *International Journal of Earth Sciences* 96,
672 613–622.

673 Pearce, J. A., Kempton, P. D. & Gill, J. B., 2007. Hf–Nd evidence for the origin and
674 distribution of mantle domains in the SW Pacific. *Earth Planet. Sci. Lett.* 260, 98–
675 114.

676 Pearce, J.A., Stern R.J., 2006. Origin of back-arc basin magmas: trace element and isotope
677 perspectives. *Back-Arc Spreading Systems: Geological, Biological, Chemical, and*
678 *Physical Interactions, Geophysical Monograph Series 166, American Geophysical*
679 *Union* 10.1029/166GM06

680 Pearce, J. A., Kempton, P. D., Nowell, G. M. & Noble, S. R., 2007. Hf–Nd element and
681 isotope perspective on the nature and provenance of mantle and subduction
682 Components in Western Pacific Arc-Basin Systems. *Journal of Petrology, Volume*
683 *40, Issue 11, November 1999, Pages 1579–1611, [https://doi-](https://doi-org.insu.bib.cnrs.fr/10.1093/etroj/40.11.1579)*
684 *org.insu.bib.cnrs.fr/10.1093/etroj/40.11.1579*

685 Pearce, J.A., 2008. Geochemical fingerprinting of oceanic basalts with applications to
686 ophiolite classification and the search for Archean oceanic crust. *Lithos* 100, 14–
687 48.

688 Peccerillo, A., Taylor, S.R., 1976. Geochemistry of Eocene calc-alkaline volcanic rocks
689 from the Kastamonu area, northern Turkey, *Contributions to Mineralogy and*
690 *Petrology* 58, 63–81.

691 Pelletier B., Calmant S., Pillet R., 1998. Current tectonics of the Tonga-New Hebrides
692 region. *Earth and Planetary Science Letters* 164, 263–276.

693 Reagan, M.K., Ishizuka, O., Stern, R.J., Kelley, K.A., Ohara, Y., Blichert-Toft, J., Bloomer,
694 S.H., Cash, J., Fryer, P., Hanan, B.B., Hickey-Vargas, R., Ishii, T., Kimura, J.I., Peate,
695 D.W., Rowe, M.C., Woods, M., 2010. Fore- arc basalts and subduction initiation in

696 the Izu-Bonin-Mariana system. *Geochemistry Geophysics Geosystems* 11, Q03X12,
697 doi:10.1029/2009GC002871.

698 Rudnick, R.L. , Fountain, D.M. , 1995. Nature and composition of the continental crust: A
699 lower crustal perspective. *Reviews of Geophysics* 33(3), DOI:
700 10.1029/95RG01302

701 Schellart, W.P., 2007. North-eastward subduction followed by slab detachment to
702 explain ophiolite obduction and Early Miocene volcanism in Northland, New
703 Zealand. *Terra Nova* 19, 211–218.

704 Schellart, W. P., Lister, G. S., Toy, V.G., 2006. A Late Cretaceous and Cenozoic
705 reconstruction of the Southwest Pacific region: Tectonics controlled by
706 subduction and slab rollback processes. *Earth-Science Reviews* 76, 191–233.

707 Sdrolias, M., Müller, R.D., Mauffret, A., Bernardel, G., 2004. Enigmatic formation of the
708 Norfolk Basin, SW Pacific: a plume influence on back-arc extension. *Geochemistry
709 Geophysics Geosystems* 5, Q06005. <http://doi.org/10.1029/2003GC000643>

710 Sevin, B., Maurizot, P., Cluzel, D., Tournadour, E., Etienne, S. Folcher, N., Jeanpert, J.,
711 Collot, J., Iseppi, M., Meffre, S., Patriat, M., 2020. Post-obduction evolution. p 147-
712 188 in Maurizot, P., Mortimer, N. (editors). *New Caledonia: geology, geodynamic
713 evolution and mineral resources*. Geological Society, London, Memoir 51.

714 Sutherland, R., Collot, J., Lafoy, Y., Logan, G.A., Hackney, R., Stagpoole, V.M., Uruski, C.I.,
715 Hashimoto, T., Higgins, K., Herzer, R.H., Wood, R.A., Mortimer, N., Rollet, N., 2010.
716 Lithosphere delamination with foundering of lower crust and mantle caused
717 permanent subsidence of New Caledonia Trough and transient uplift of Lord
718 Howe Rise during Eocene and Oligocene initiation of Tonga-Kermadec subduction,
719 western Pacific. *Tectonics* 29, TC2004. <http://doi.org/10.1029/2009TC002476>

720 Tanaka, T., Togashi, S., Kamioka, H., Amakawa, H., Kagami, H., Hamamoto, T., Yuhara, M.,
721 Orihashi, Y., Yoneda, S., Shimizu, H., Kunimaru, T., Takahashi, K., Yanagi, T.,
722 Nakano, T., Fujimaki, H., Shinjo, R., Asahara, Y., Tanimizu, M., Dragusanu, C., 2000.

723 JNdi-1: a neodymium isotopic reference in consistency with La Jolla neodymium.
724 Chemical Geology 168, 279–281.

725 Timm, C., Hoernle, K., Werner, R., Hauff, F., van den Bogaard, P., White, J., Mortimer, N.,
726 Garbe-Schönberg, D., 2010. Temporal and geochemical evolution of the Cenozoic
727 intraplate volcanism of Zealandia. Earth-Science Reviews 98, 38–64.

728 Timm, C., de Ronde, C.E.J., Hoernle, K., Cousens, B., Wartho, J.-A., Caratori Tontini, F.,
729 Wysoczanski, R., Hauff, F., Handler, M., 2019. New age and geochemical data from
730 the southern Colville and Kermadec ridges, SW Pacific: insights into the recent
731 geological history and petrogenesis of the proto-Kermadec (Vitiáz) Arc. Gondwana
732 Research 72, 169–193.

733 Todd, E., Gill, J. B., Wysoczanski, R. J., Handler, M. R., Wright, I. C., and Gamble, J. A., 2010.
734 Sources of constructional cross-chain volcanism in the southern Havre Trough:
735 New insights from HFSE and REE concentration and isotope systematics, *Geochem.*
736 *Geophys. Geosyst.*, 11, Q04009, doi:10.1029/2009GC002888.

737 Todd, E., Gill, J.B., Wysoczanski, R.J., Hergt, J., Wright, I.C., Leybourne, M.I., Mortimer, N.,
738 2011. Hf isotopic evidence for small-scale heterogeneity in the mode of mantle
739 wedge enrichment: southern Havre Trough and South Fiji Basin back arcs.
740 *Geochemistry, Geophysics, Geosystems* 12, Q09011.
741 <https://doi.org/10.1029/2011GC003683> .

742 Todd, E., Gill, J.B., Pearce, J.A., 2012. A variably enriched mantle wedge and contrasting
743 melt types during arc stages following subduction initiation in Fiji and Tonga,
744 southwest Pacific. *Earth and Planetary Science Letters* 335–336, 180–194.

745 Todt, W., Cliff, R.A., Hansen, A., Hofmann, A., 1996. Evaluation of a 202Pb-205Pb double
746 spike for high-precision isotope analysis. In: *Earth Processes: Reading the Isotopic*
747 *Code* (Eds: A. Basu, S.R. Hart). American Geophysical Union Geophysical
748 Monograph 95, 429–437.

749 Turner, S. J. & Langmuir, C. H. 2015, The global chemical systematics of arc front
750 stratovolcanoes: evaluating the role of crustal processes. *Earth Planet. Sci. Lett.*
751 **422**, 182–193.

752 Whattam, S.A., Malpas, J., Smith, I.E.M., Ali, J.R., 2006. Link between SSZ ophiolite
753 formation, emplacement and arc inception, Northland, New Zealand: U–Pb
754 SHRIMP constraints; Cenozoic SW Pacific tectonic implications. *Earth and*
755 *Planetary Science Letters* 250, 606–632

756 Vervoort, J. D., Patchett, P. J., Blichert-Toft, J. & Albarède, F., 1999. F. Relationships
757 between Lu–Hf and Sm–Nd isotopic systems in the global sedimentary system.
758 *Earth Planet. Sci. Lett.* **168**, 79–99.

759

760 Yang A. Y., Langmuir C. H., Cai, Y. , Michael, P., Goldstein, S. L., and Chen, Z. 2021, A
761 subduction influence on ocean ridge basalts outside the Pacific subduction shield.
762 *Nature Communications* volume 12, Article number: 4757

763

764

765 **Figure captions**

766

767 **Fig. 1. A.** Study area in the SW Pacific Ocean. LR: Loyalty ridge, TKR: Three King's ridge,
768 NR: Norfolk Ridge, BG: Bougainville Guyot. **B.** Dredge sample location map and major
769 bathymetric features of ridge and basins. The symbol colour code is established by
770 geochemical signatures as justified in Figs. 3-5: Blue circles=tholeiitic basalts and
771 basaltic andesites, yellow hexagons=incompatible element-enriched lavas. **C.** Sample
772 location depths projected onto two NW-SE seismic profiles across the Loyalty and Three
773 Kings ridges (from Mortimer and Patriat, 2016).

774

775 **Fig. 2.** Major element compositions of Loyalty and Three Kings ridge area lavas plotted
776 on an anhydrous basis. **A.** total alkali – silica plot (Le Bas et al., 1986). **B.** K₂O vs SiO₂ plot
777 (Peccerillo and Taylor, 1976). The symbol colour code is established by geochemical
778 signatures as justified in Figs. 3-5: Blue circles=tholeiitic basalts and basaltic andesites,
779 yellow hexagons=incompatible element-enriched lavas.

780

781 **Fig 3.** A-D: Multi-element normalised plots of samples from Loyalty and Three Kings
782 ridge area. **A-C.** Rare-earth element (REE) patterns normalized to CI Chondrite
783 (McDonough and Sun, 1995). **D.** Multielement plot of all samples normalized to
784 primitive mantle values (McDonough and Sun, 1995). **A.** the two most depleted BABB-
785 like tholeiitic samples DR39A and DR39. **B.** transitional tholeiitic basalts (blue circles). **C.**
786 incompatible trace element-enriched samples (yellow hexagons). For reference, the
787 transitional compositions are shown as thin blue lines in panels A and C. **E.** Th/Yb vs
788 Nb/Yb diagram of Pearce (2008). Fields of back-arc basalts (BABB) and Island arc
789 basalts (IAB) are those of Li et al. (2015).

790

791 **Fig. 4. A.** Pb isotopic composition of VESPA samples, most of the samples lie above the
792 North Hemisphere Reference Line (NHRL, Hart, 1984); **B.** ϵ_{Hf} and Sr isotopes vs ϵ_{Nd} . The
793 dotted black line represents the mantle array of Vervoort et al (1999). The green areas
794 represent MORB from the South West Indian ridge and the grey areas MORB from the
795 Pacific (The data were downloaded from the PetDB Database
796 (www.earthchem.org/petdb on 16 August, 2022, using the following parameters:
797 feature name = SPREADING CENTER/ EAST PACIFIC RIDGE, PACIFIC-NAZCA RIDGE,
798 PACIFIC IZANAGI RIDGE, PACIFIC-ANTARCTIC RIDGE, SOUTHWEST INDIAN RIDGE and
799 rock classification= « basalt.”). The blue dotted lines identify the Indian/Pacific Mantles
800 limits as defined by Pearce et al. (1999) and Pearce et al. (2007).

801

802 **Fig.5:** Hf, Nd and Sr isotope ratios vs $^{206}\text{Pb}/^{204}\text{Pb}$. In the left column, VESPA samples are
803 compared with various other reference sets. Two isotopic trends shown by purple and
804 pink bands, are less well defined with Sr isotopes, possibly due to the sensitivity of this
805 system to sea water alteration. The enriched-Pacific-MORB trend crosscuts the EM2
806 trend at one extremity, suggesting a pseudo binary mixing pattern (e.g. Douglas and
807 Schilling, 2000). C.F.Z. = Cook Fracture Zone, TKR.=Three Kings Ridge. The green and
808 grey areas correspond to SW Indian and Pacific MORB respectively (see Fig. 4 for
809 references). The purple fields represent Kermadec Subducting Sediments (Todd et al,
810 2010). Red circles are South Fiji basin basalts (Mortimer et al., 1998; Todd et al., 2011)
811 and blue circles are Kermadec basalts (Todd et al., 2010).

812

813 **Fig 6. A.** Variation in sample longitude, Hf isotope ratios and La/Sm ratios with age. **B.**
814 Variations in sample Hf isotope ratios and La/Sm ratios with sample depth. See Fig. 4 for
815 symbols. With one exception, all enriched samples were collected at shallower depths
816 than tholeiitic samples. N.R.=Norfolk Ridge, L.R.=Loyalty Ridge, T.K.R.=Three Kings
817 Ridge. Norfolk Ridge samples from Mortimer et al. (2021).

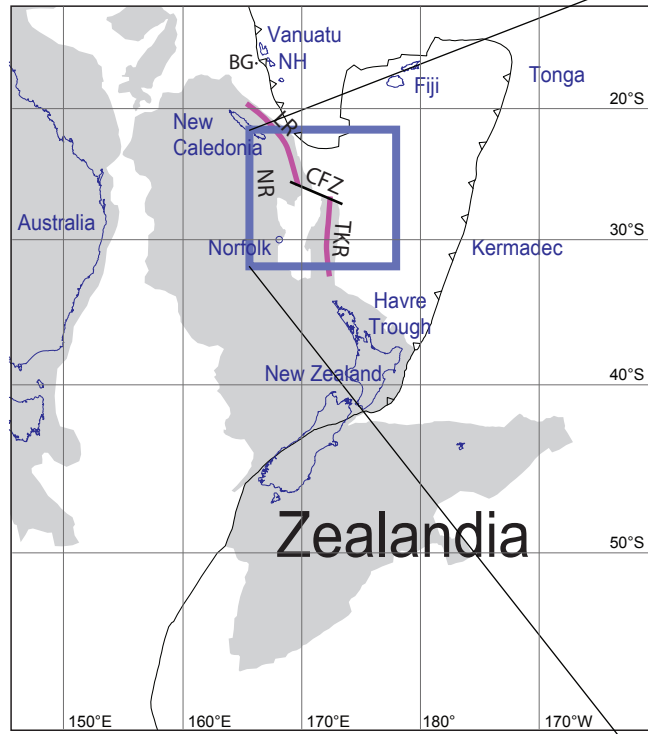
818

819 **Fig. 7.** Speculative geodynamic reconstruction to explain the development of the Loyalty
820 and Three Kings ridges along the eastern Zealandian margin. Our data demonstrate the
821 building of the Loyalty-Three Kings Ridge is achieved by arc volcanism over a very short
822 (3 Myr) Late Oligocene-Early Miocene period of time (24-22 Ma, panel C). See details in
823 the text. **A.** Late Eocene-Early Oligocene jamming of the Eocene subduction zone
824 (Maurizot et al, 2020a). Subdued or no volcanic activity accompanying collision and
825 obduction. **B.** Post-orogenic extension and resumption of subduction. Extension induces
826 thinning of the previously thickened lithosphere at the same time as emplacement of the
827 Oligocene granitoids of New Caledonia. **C.** Maturing subduction and trench rollback
828 result in decompression melting of the normal Pacific upper mantle to produce low-K

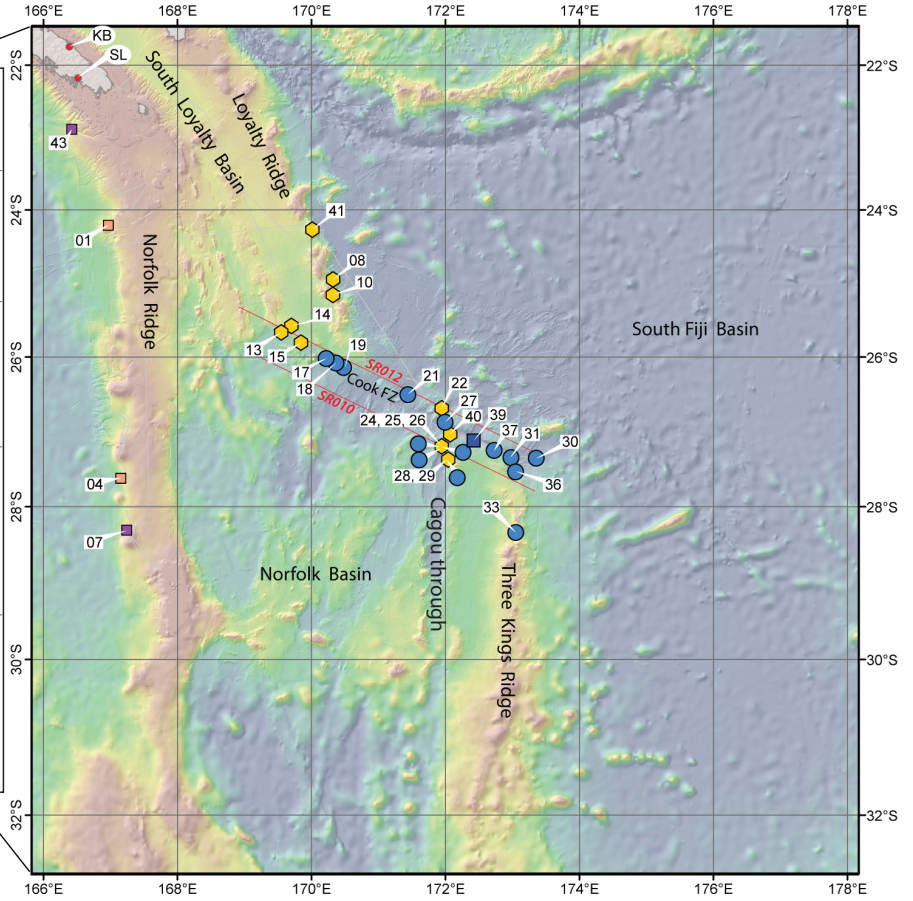
829 tholeiites. Later, there is mature arc formation. As the retreating Pacific slab steepens,
830 there is a significant increase of slab derived fluid input into the wedge, which produces
831 the high-K to shoshonitic lavas. The topographic ridges/arcs are built during this phase.
832 **D.** Cessation of volcanism at Loyalty-Three Kings ridges. Slab retreats rapidly driving arc
833 volcanism east of the Loyalty-Three Kings Ridge. The arc later stabilises along the Lau-
834 Colville Ridge and, eventually the Kermadec-Tonga Ridge. NC: New Caledonia, L3KR:
835 Loyalty-Three Kings Ridge, LCR: Lau-Colville Ridge, SFB: South Fiji Basin.

Fig. 1

A



B



C

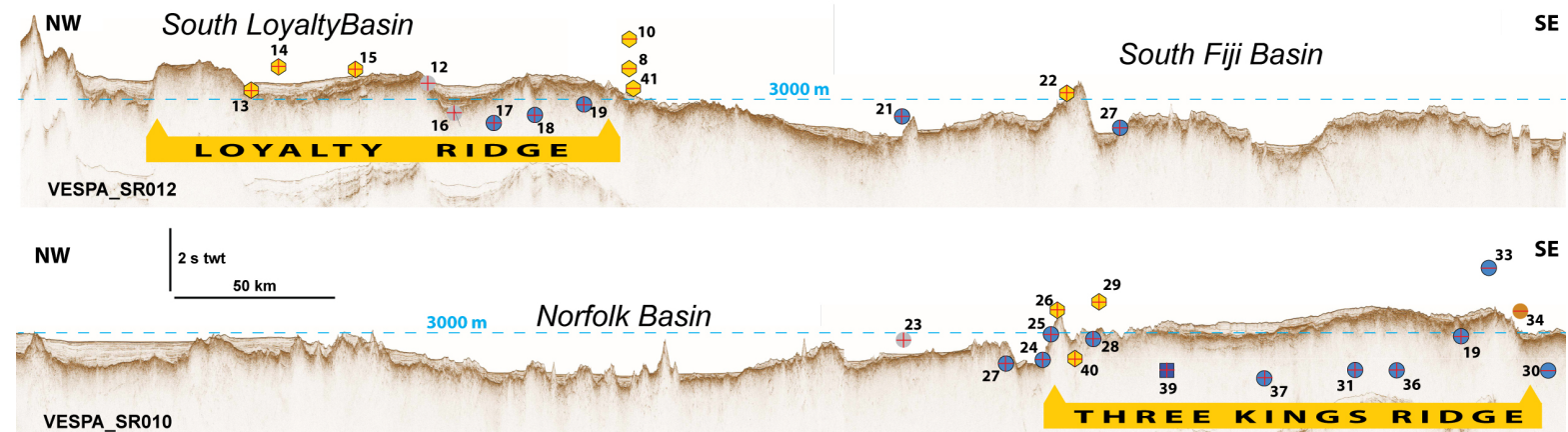


Fig. 2

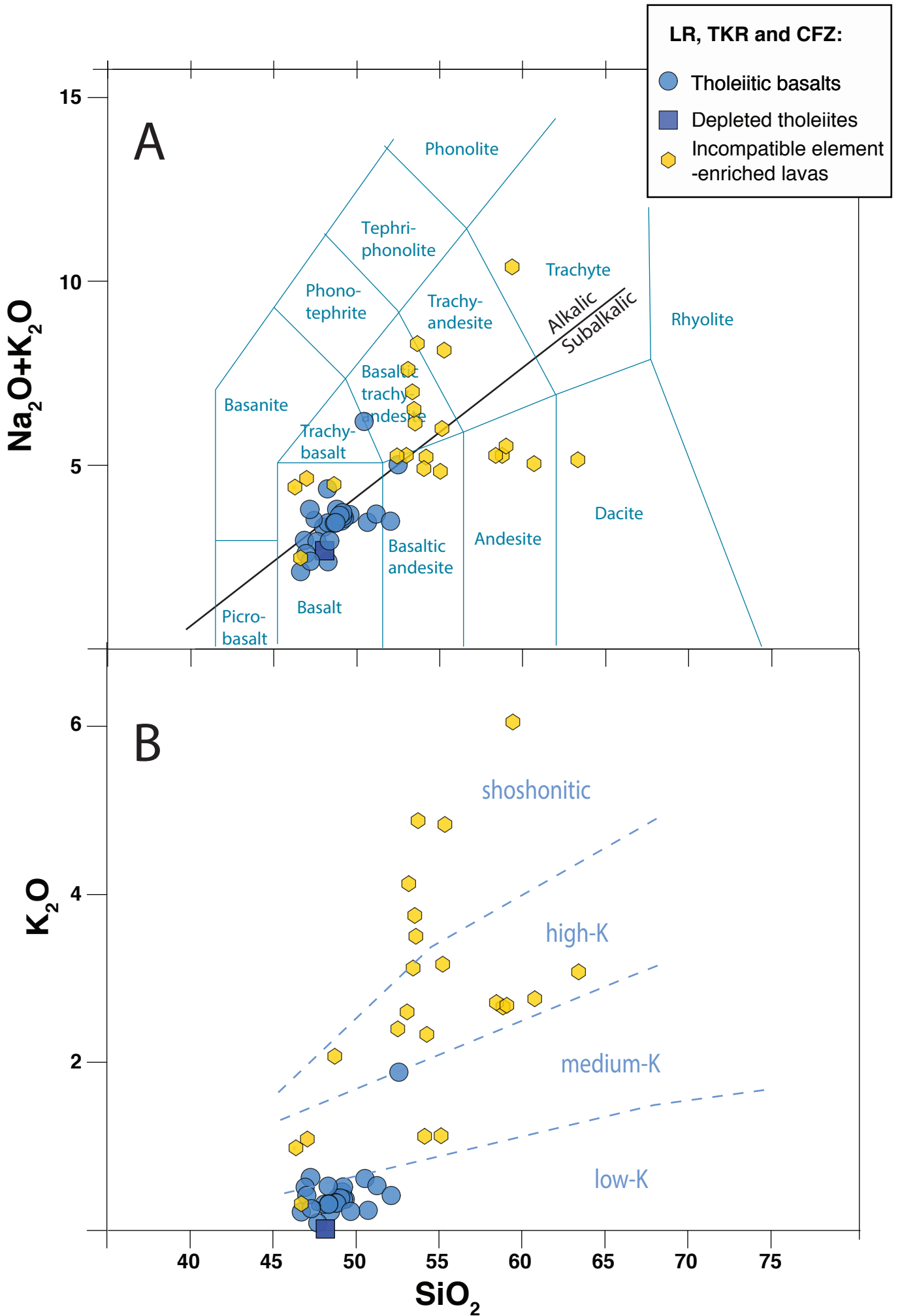


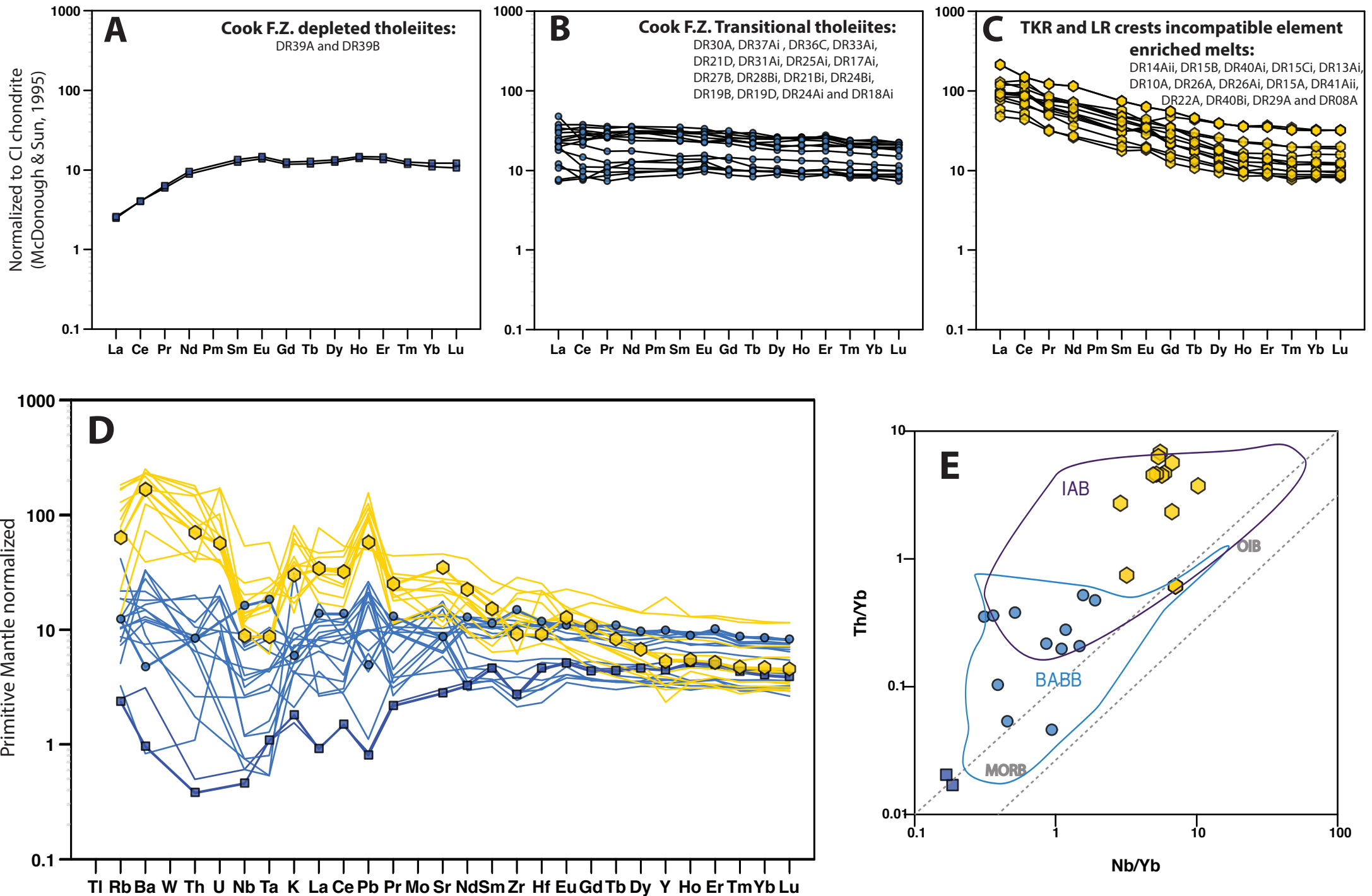
Fig. 3

Fig.4

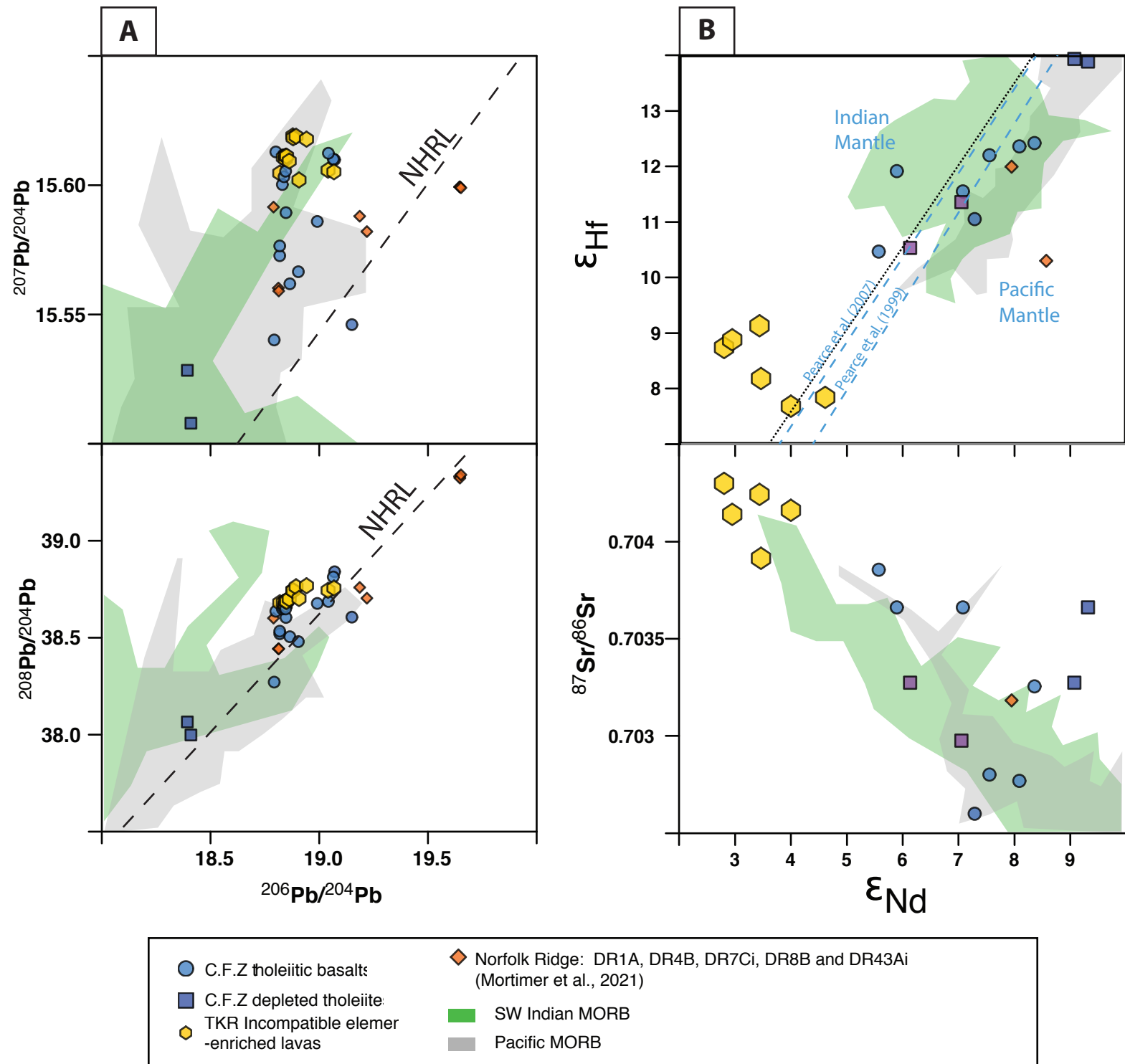


Fig. 5

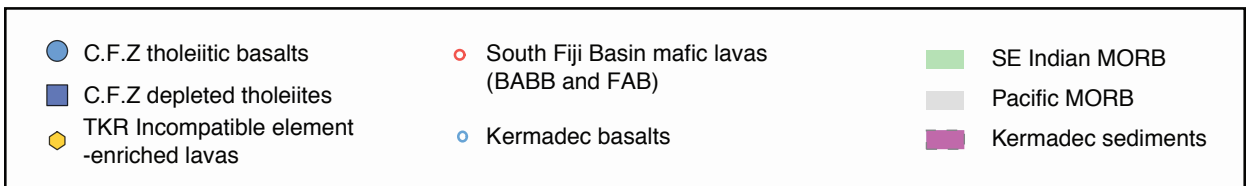
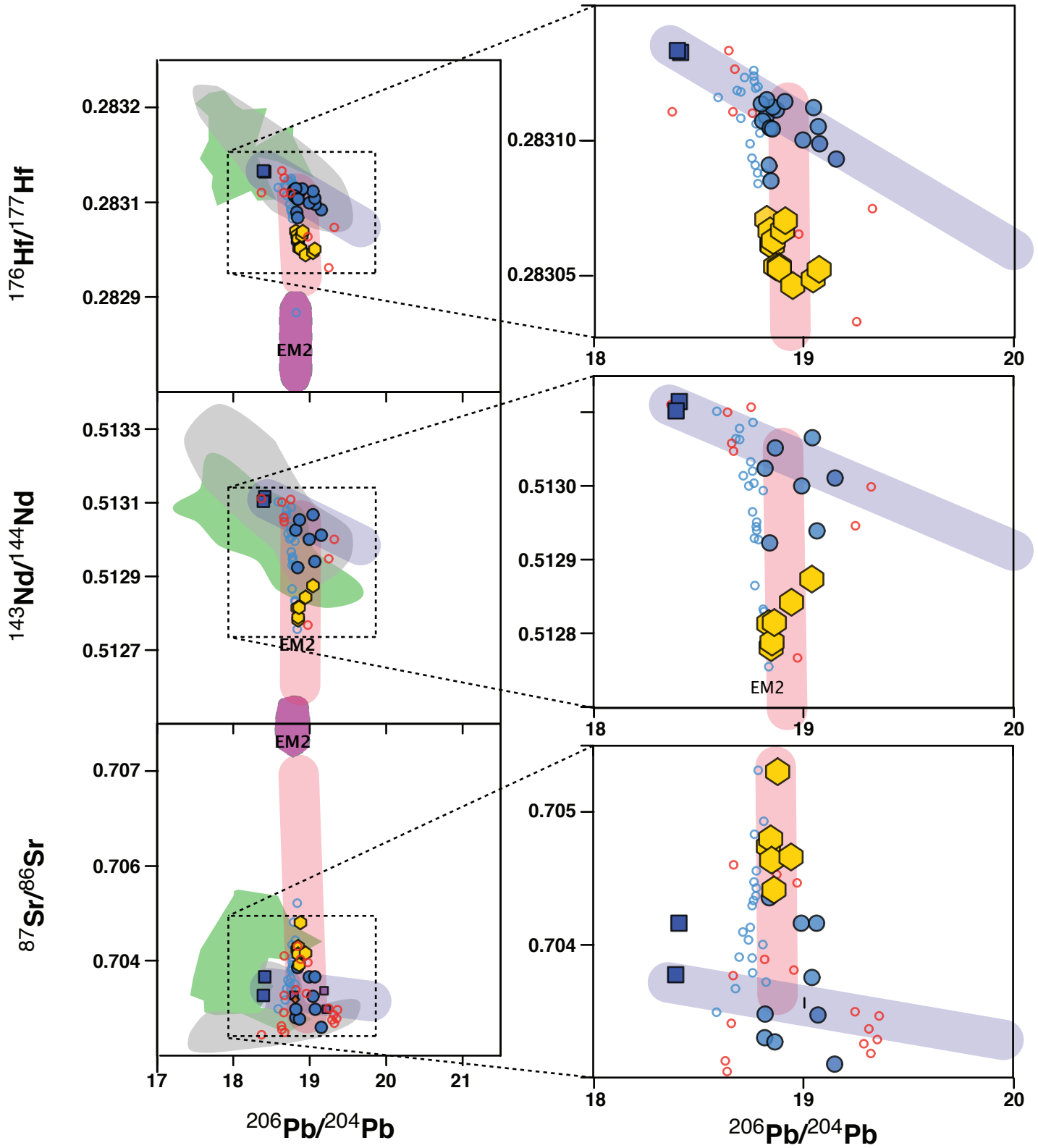
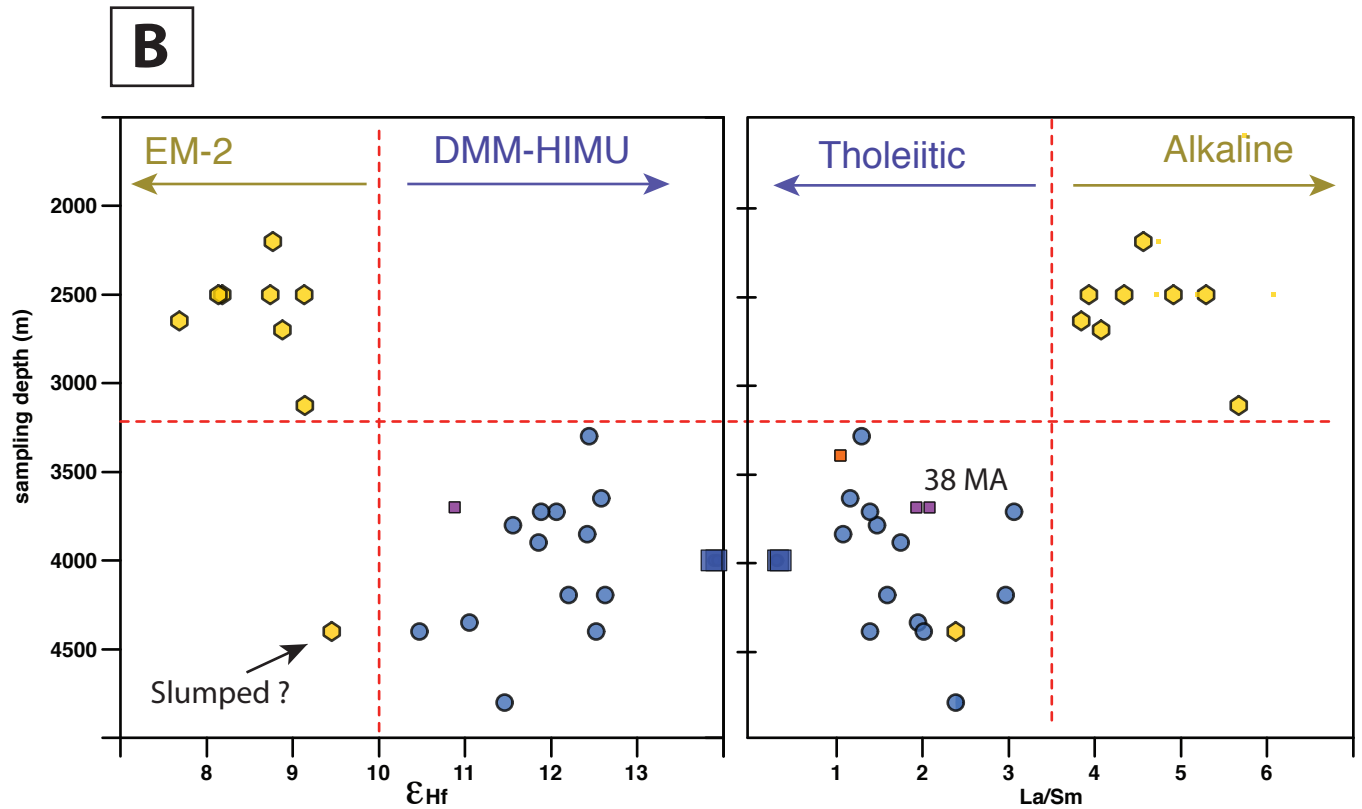
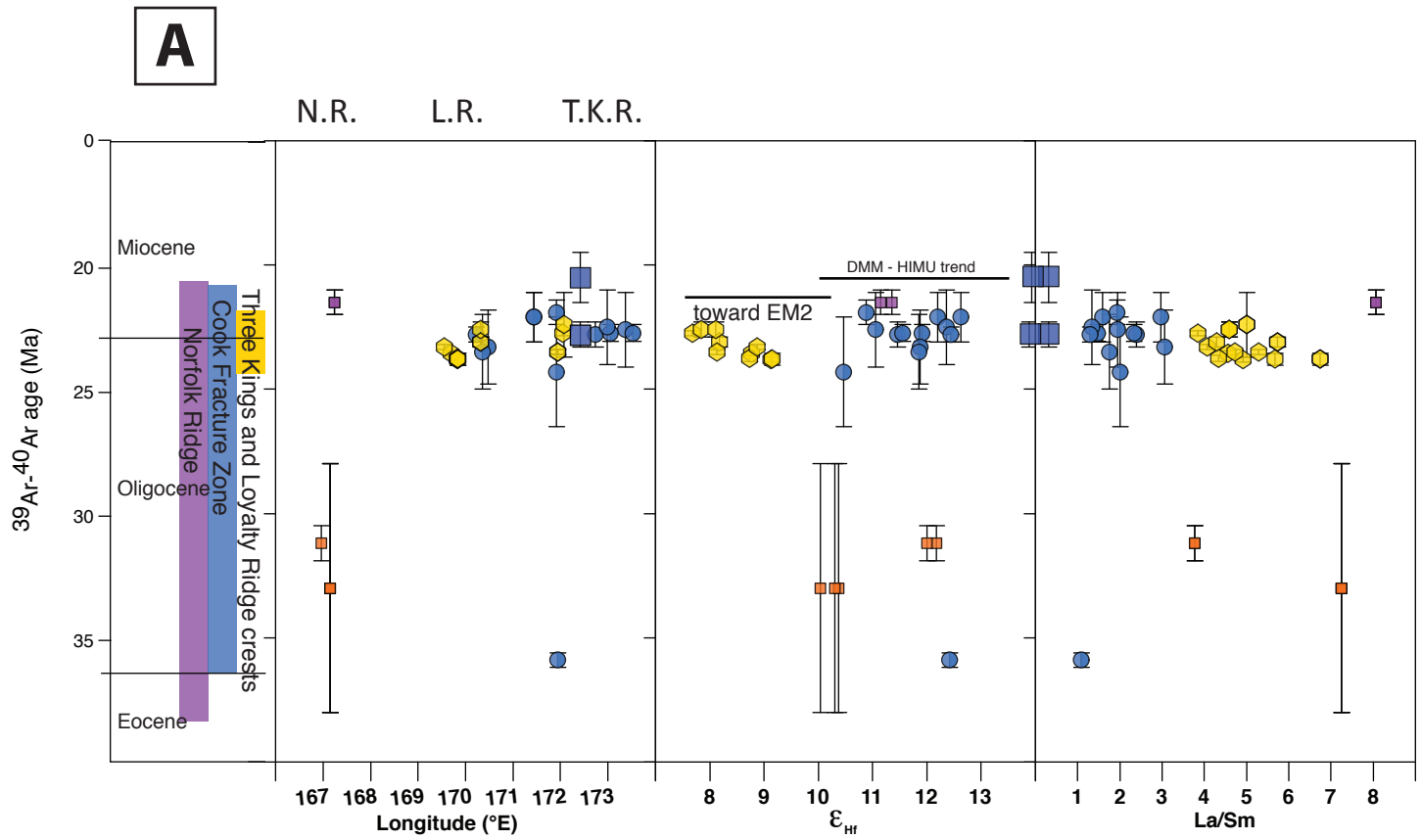
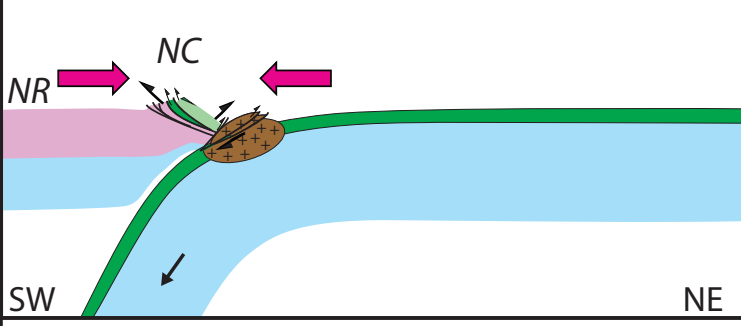


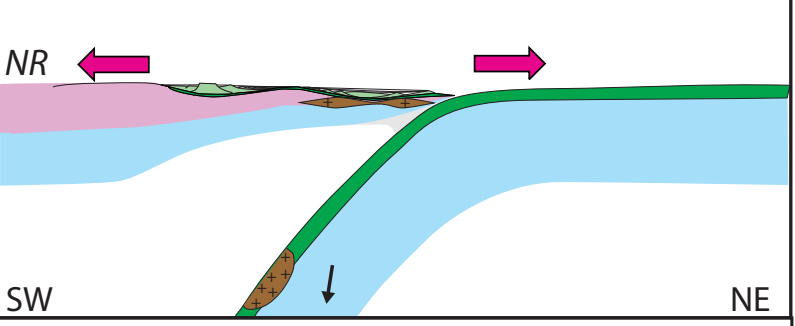
FIGURE 6



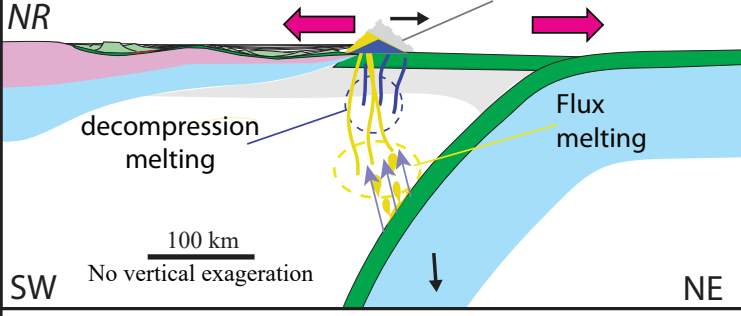
A Closure of Eocene Subduction
Obduction in New Caledonia ~ 34 Ma
Maurizot et al. (2020a)



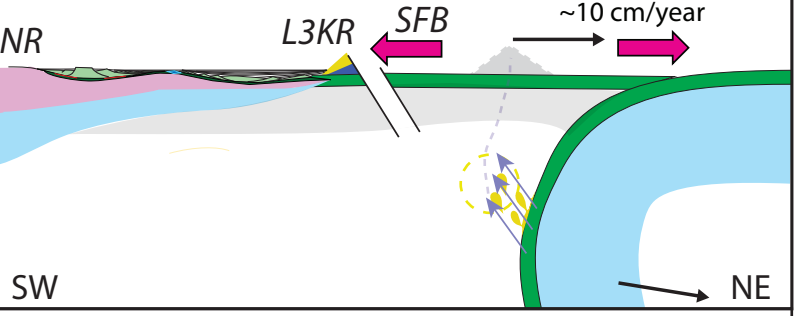
B Post-Orogenic Extension
& Resumption of Subduction 32-25 Ma








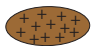
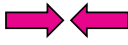


C Arc formation 25-22 Ma
(This paper)



D Trench retreat acceleration After 22 Ma



	Continental crust		>50 Ma lithospheric mantle		Sediment melts
	Oceanic crust		Other mantle : asthenosphere and young lithosphere (dark grey)		Motion of slab and arc relative to Norfolk Ridge
	Peridotite Nappe of New Caledonia				
	Buoyant crust : oceanic plateau or continental crust				Compression (or extension) resulting from convergence (or divergence) between NR and the subduction front